BFSN #1253000, VOL 0, ISS 0

Computer simulation for improving radio frequency (RF) heating uniformity of food products: A review

Zhi Huang, Francesco Marra, Jeyamkondan Subbiah, and Shaojin Wang

QUERY SHEET

This page lists questions we have about your paper. The numbers displayed at left can be found in the text of the paper for reference. In addition, please review your paper as a whole for correctness.

There are no Editor Queries in this paper.

TABLE OF CONTENTS LISTING

The table of contents for the journal will list your paper exactly as it appears below:

Computer simulation for improving radio frequency (RF) heating uniformity of food products: A review
Zhi Huang, Francesco Marra, Jeyamkondan Subbiah, and Shaojin Wang

CRITICAL REVIEWS IN FOOD SCIENCE AND NUTRITION
2017, VOL. 0, NO. 0, 1–25
http://dx.doi.org/10.1080/10408398.2016.1253000

Taylor & Francis
Taylor & Francis Group

Computer simulation for improving radio frequency (RF) heating uniformity of food products: A review

Zhi Huang[a], Francesco Marra[b], Jeyamkondan Subbiah[c], and Shaojin Wang[a,d]

[a]College of Mechanical and Electronic Engineering, Northwest A&F University, Yangling, Shaanxi, China; [b]Dipartimento di Ingegneria Industriale, Università degli studi di Salerno, Fisciano, SA, Italy; [c]Departments of Biological Systems Engineering and Food Science & Technology, University of Nebraska-Lincoln, Lincoln, Nebraska, USA; [d]Department of Biological Systems Engineering, Washington State University, Pullman, Washington, USA

ABSTRACT

Radio frequency (RF) heating has great potential for achieving rapid and volumetric heating in foods, providing safe and high-quality food products due to deep penetration depth, moisture self-balanceeffects, and leaving no chemical residues. However, the nonuniform heating problem (usually resulting in hot and cold spots in the heated product) needs to be resolved. The inhomogeneous temperature distribution not only affects the quality of the food but also raises the issue of food safety when the microorganisms or insects may not be controlled in the cold spots. The mathematical modeling for RF heating processes has been extensivelystudied in a wide variety of agricultural products recently. This paper presents a comprehensive review of recent progresses in computer simulation for RF heating uniformity improvement and the offered solutions to reduce the heating nonuniformity. It provides a brief introduction on the basic principle of RF heating technology, analyzes the applications of numerical simulation, and discusses the factors influencing the RF heating uniformity and the possible methods to improve heating uniformity. Mathematical modeling improves the understanding of RF heating of food and is essential to optimizethe RF treatment protocol for pasteurization and disinfestation applications. Recommendations for future research have been proposed to further improve the accuracy of numerical models, by covering both heat and mass transfers in the model, validating these models with sample movement and mixing, and identifying the importantmodelparameters by sensitivity analysis.

KEYWORDS

Computer simulation; food products; heating uniformity; model; radio frequency

1. Introduction

Radiofrequency (RF) heating (also known as capacitive dielectric heating) is a recognized rapid electro-heating technology, which forms a part of innovative techniques based on electromagnetic heating and other nonthermal methods. The available systems for producing and transferring RF power to dielectric heating can be divided into two distinct groups: the more widespread conventional RF healing equipment and the more recent 50-Ω RF heating equipment (Marchand and Meunier, 1990). Whether conventional or 50-Ω dielectric heating systems are used, the RF applicator has to be designed for the particular product being heated. Although the size and shape of the applicator can vary enormously, they mostly fall into one of three main types: the through field applicator, the fringe field applicator, and the staggered through field applicator (Jones and Rowley, 1996). Conceptually, a through field RF applicator (with a pair of parallel plates) is the simplest and the most common design of RF applicators in which the lossy material is placed between the two electrodes to form a parallel plate capacitor. This type of applicator is mainly used for heating bulk materials or related large and thick objects. High voltage is applied onto one of the electrodes while the other is grounded, thus causing propagation of electromagnetic waves between the electrodes. During RF treatments, heat is generated within the product due to molecular friction resulting from oscillating dipole molecules and migrating ions caused by the applied alternating electric field (Piyasena et al., 2003). Theoretically, therefore, RF heating is expected to deliver more uniform heat at a faster rate than conventional heating. Conventional heating relies on conduction and convection to transport heat from the heating sources to the product, which requires relatively longer period of time, whereas RF heating has the potential to deliver heat instantly throughout the product (Zhao et al., 2000). RF heating offers the advantages of providing more uniform heating over sample geometry than microwave heating does due to deeper wave penetration into the sample and is more economical than microwave at higher power levels (Luechapattanaporn et al., 2004). These features of RF heating have generated great interests for applications in the food-processing industry.

The potential use of RF technology for food processing was recognized since the 1940s (McCormick, 1988). These early efforts employed RF energy for applications, such as the cooking of processed meat products, heating of bread, dehydration, and blanching of vegetables at 150 MHz (Moyer and Stotz, 1947). The next generation of commercial applications for RF energy in the food industry was postbake drying of cookies and

CONTACT Shaojin Wang, Ph.D, Professor shaojinwang@nwsuaf.edu.cn College of Mechanical and Electronic Engineering, Northwest A&F University, Yangling, Shaanxi 712100, China.

Color versions of one or more of the figures in the article can be found online at www.tandfonline.com/bfsn.

a) Nomenclature

A	plate area of an electrode (m^2)
$\vec{B}$	magnetic flux density (dimensionless)
c	speed of light in free space (3×10^8 m/s)
C	capacitance (F)
c_p	heat capacity (J/kg K)
c_e	empirical constantin Eq. (32) (J/kgK)
d	plate distance between the two electrodes (m)
d_p	penetration depth (m)
D	empirical constants in Eq. (32) ($J/K^n kg$)
$\vec{D}$	electric flux density (dimensionless)
$\vec{E}$	electric field vector (dimensionless)
E	electric field intensity (V/m)
h	overall external convective heat transfer coefficient (W/m^2K)
$\vec{H}$	magnetic field intensity (dimensionless)
f	frequency (Hz)
I_C	electric current (A)
$\vec{J}$	current density (dimensionless)
k	thermal conductivity (W/mK)
k_e	empirical constantin Eq. (33) (W/mK)
m_w	evaporating flux of water (kg/m^2 s)
n	empirical constants in Eq. (32) (dimensionless)
$\vec{n}$	normal vector of the sample surface (dimensionless)
P	power density generated by electric field (W/m^3)
S_d	changes in density per unit change in temperature (kg/m^3 K)
S_k	changes in thermal conductivity per unit change in temperature (W/mK^2)
t	time (s)
T	sample temperature (K)
$\tan\delta$	dielectric loss tangent (dimensionless)
$\partial T/\partial t$	temperature rate of change (K/s)
V	electric potential (V)
V_{vol}	material volume (m^3)
ω	angular frequency (rad/s)
SD	standard deviation
δ	dielectric loss angle (rad)
ε	permittivity (dimensionless)
ε_0	free space permittivity (F/m)
ε'	dielectric constant (F/m)
ε''	dielectric loss factor (F/m)
ε_r	relative permittivity (dimensionless)
ε_r'	relative dielectric constant (dimensionless)
ε_r''	relative dielectric loss factor (dimensionless)
∇	gradient operator
λ	latent heat of vaporization per unit mass of evaporated water (J/kg)
μ	magnetic permeability (H/m)
ρ	density (kg/m^3)
ρ_e	empirical constant in Eq. (31) (kg/m^3)
σ	electrical conductivity (S/m)

b) Subscripts

a	air
av	average
i	insect
mat	food material
p	product
s	solid
sh	initial freezing point
sw	normal freezing point of pure water

snack foods, which began in the late 1970s (Holland, 1974). Later in 1990s, the area of RF pasteurization was studied with attempts made to improve energy efficiency and solve technical problems (Zhao et al., 2000). This in turn has led to recent investigations on RF heating applications in food processing, as well as dielectric properties of the product and system specific factors that influence the RF heating (Piyasena et al., 2003). Subsequently, Marra et al. (2009) and Jojo and Mahendran (2013) reviewed several additional applications for RF heating in food processing and their impacts on general quality aspects of foods. The most recent focus of this novel heating technology was investigated for baking and roasting (Awuah et al., 2014a), cooking (Kirmaci and Singh, 2012; Laycock et al., 2003; Marra et al., 2007; Rincon et al., 2015), controlling insects (Hou et al., 2016; Jiao et al., 2012; Wang et al., 2007a, b), defrosting (Farag et al., 2009; Llave et al., 2014, 2015), drying (Jumah, 2005; Wang et al., 2011, 2014), pasteurization (Awuah et al., 2005; Gao et al., 2011; Geveke et al., 2002; Ha et al., 2013; Kim et al., 2012; Liu et al., 2011; Nagaraj et al., 2016), sterilization (Guan et al., 2004; Wang et al., 2003b), thawing (Farag et al., 2008a, 2011; Uyar et al., 2015), and many more.

Although there are many research evidences suggesting possible advantages in the food industry, RF energy has not yet been exploited to its fullest potential in the industrial applications. One of the major drawbacks of RF heating is the existence of hot spots in several zones depending on product geometry (Alfaifi et al., 2014; Fu, 2004; Tiwari et al., 2011b; Wang et al., 2006b; Wang et al., 2008a). Sample size, shape, and nonhomogeneous dielectric properties (DPs) could result in nonuniform electric field distribution, which in turn causes nonuniform temperature distribution (Birla et al., 2008a; Marra et al., 2007; Tiwari et al., 2011a). The nonuniform temperature distribution has been studied in different agricultural commodities, such as dry nuts (Wang et al., 2001, 2002, 2005; Wang et al., 2014), dried fruits (Alfaifi et al., 2014), eggs (Lau et al., 2016), fresh fruits (Birla et al., 2004, 2005; Tiwari et al., 2008; Wang et al., 2006a), legumes (Huang et al., 2015c; Jiao et al., 2011; Wang et al., 2008c, 2010) and meat (Llave et al., 2015; Marra et al., 2007; Romano and Marra, 2008; Uyar et al., 2014, 2016). Major problems in RF heating, such as poor end quality, pathogens/insects survivals, microbial safety concerns, and overheating, are related to nonuniform heating during RF treatment (Birla et al., 2004; Brunton et al., 2005; Jiao et al., 2012; Kim et al., 2012; Kirmaci and Singh, 2012). Several researchers have studied the temperature distribution during RF heating in food materials and suggested measures to reduce the nonuniform temperature distribution (Chen et al., 2015b; Huang et al., 2016b; Ikediala et al., 2002; Jiao et al., 2014a; Tiwari et al., 2011a). The trial and error procedures are time consuming, costly, and often provide limited information. Due to rapid progress in computing capability, computational modeling has increasingly been used to predict RF power and temperature

distribution in food products without the necessity of extensive experiments.

Numerical techniques, such as the finite element method (FEM), have been extensively used in simulations of RF heating. Its capability was first investigated by Baginski et al. (1989) and again later by Choi and Konrad (1991). Starting from the mid 1990s, a number of papers have appeared in the literature and have discussed mathematical modeling and the computer simulation of RF systems. Neophytou and Metaxas (1996, 1997, 1998, 1999) attempted to model the electrical field for industrial-scale RF heating systems and compared solutions from both electrostatic and wave equations. Later on, Marra et al. (2007) proposed and experimentally validated a mathematical model for RF heating of solid-like food (meat batter), based on so-called quasi-static approach, where the Gauss law was coupled with classical transient heat transfer equation, taking into account, beside the conductive term, a volumetric power generation. After that, further steps towards improving the understanding of RF heating were taken for various food products, such asdry foods (Huang et al., 2016a; Jiao et al., 2015a; Tiwari et al., 2011a, b), fruits (Birla et al., 2008a, b), meat lasagna (Wang et al., 2012), peanut butter (Jiao et al., 2014a, b), and raisins (Alfaifi et al., 2014). Overall, the consensus is that RF heating is only able to heat certain food products uniformly, and sometimes processing aids (Jiao et al., 2015b) or modifications to the RF applicator (Tiwari et al., 2011a) are needed to achieve good RF heating uniformity. These include hot water-assisted treatment (Tiwari et al., 2008), combining with moving or rotating method (Birla et al., 2008a; Chen et al., 2016), intermittent mixing (Chen et al., 2015b), electrode type modification (Tiwari et al., 2011a), and similar dielectric material surrounding methods (Huang et al., 2015c; Jiao et al., 2015b).

The general purpose of this paper was to review the current state of numerical modeling of overheating that usually occurs at corners and edges of the RF-treated products in rectangular containers for better understanding the causes of nonuniform temperature distributions in foods and provide an optimal solution for improving the RF heating uniformity in these foods. The prospects of further research were examined and various applications of numerical models were discussed. The specific objectives of this review were (1) to introduce the basic mechanism of RF heating and present the fundamental of mathematical modeling of RF heating, (2) to review the literatures of computer simulation on RF heating applications in food processing, (3) to explore the nonuniform RF heating behavior with the developed simulation model, (4) to analyze the main factors that affect the RF heating uniformity and discuss the simulated methods to improve RF heating uniformity in food processing, and (5) to propose recommendations for developing computer aided engineering of RF processes on an industrial-scale.

2. Overview of RF heating modeling

2.1. RF heating system

RF technology uses electromagnetic energy within a frequency range of 3 kHz to 300 MHz to heat target foods. Federal Communication Commission (FCC) assigned 13.56 ± 0.00678, 27.12 ± 0.16272, and 40.68 ± 0.02034 MHz for RF treatments in industrial, scientific and medical (ISM) applications to prevent disturbance in telecommunications (Jones and Rowley, 1996). RF heating is based on the transformation of alternating electromagnetic field energy into thermal energy by affecting the polar molecules and charged ions of a material. Dielectric materials are composed of atoms or molecules irrespective of its phase (solid, liquid, or gas) and atoms or molecules are composed of negatively charged electrons and positively charged nucleus. These constituents may belocked into regular structures of crystals or free to wander through the structure. Therefore, several types of electric displacements of these constituents, such as electronic, atomic, molecular, and ionic, are possible (Hartshorn, 1949). The molecular displacement involves molecules that are initially asymmetrical in structure and have a definite electric moment in addition to their own electric field when placed in an external electric field (Piyasena et al., 2003). When an external electric field is applied, the bipolar molecules tend to behave like microscopic magnets and attempt to align themselves with the field. When the electrical field is changing millions of times per second (e.g. 27.12 MHz), these molecular magnets are unable to withstand the forces acting to slow them. This resistance to the rapid movement of the bipolar molecules creates friction and results in heat dissipation in the material exposed to the RF radiation. This interaction results in translation motions of free or bound charges and rotation of dipoles, and causes losses that, in turn, produce the volumetric heating (Piyasena et al., 2003). The ability of RF radiation to penetrate and couple with materials provides an attractive method for obtaining controlled and precise heating.

In RF treatment, heat is generated throughout the material by molecular friction in high-frequency alternating electric fields, leading to faster heating rates, which was similar to the microwave (MW) heating (Tang et al., 2005). Both RF and MW heating methods are nonionizing radiation since the frequencies in RF and MW ranges cannot produce sufficient energy to ionize molecules (Awuah et al., 2014b). Therefore, RF and MW heating is also called dielectric heating or dielectric loss heating. RF and MW systems have been recognized to be 50–70% heating efficient in comparison to 10% efficiency with conventional heating ovens (Mermelstein, 1997). RF heating also differs from the higher frequency MW heating (915 MHz and 2450 MHz). In RF heating, the electrical field is commonly generated in a directional manner between a pair of electrode plates, but the electrical field could approach the product from all directions in MW heating depending on different mode designs. RF and MW system configurations are totally different, since MW energy is generated by special oscillator tubes, magnetrons or klystrons, and can be transmitted to an applicator or antenna through a waveguide or coaxial transmission line. The output of such tubes tends to be in a range from 0.5 to 100 kW and requires a special power supply (Piyasena et al., 2003). RF systems are generally simpler to construct than MW systems, which usually contain an oscillator and applicator circuit. The RF heating also offers simple uniform field patterns as opposed to the complex nonuniform standing wave patterns in a MW oven (Piyasena et al., 2003). Compared with MW energy, RF energy has the advantage of heating bulk food because of its

relatively longer wavelength (7.4–22.1 m in vacuum). As a result, a better heating pattern for RF processing would be obtained compared to MW processing.

A typical RF system consists of two main components: generator and applicator. The generator part is mainly used to generate the RF energy, and the applicator is a metal structure, which directs the RF field to the product or load to be heated. Two main kinds of RF systems are used in commercial applications: the open circuit (also called free running oscillator) and the 50 Ω technology based on their wave generation mechanisms, components, and properties (Marra et al., 2009). The open circuit RF system is used widely in many industrial applications, but the 50-Ω system is a relatively new technology to provide a fixed frequency compared to self-oscillatory circuit, and also to precisely control power and feedback (Jones and Rowley, 1996). Thus the heating rate can be tightly controlled and precise final temperatures can be achieved easily in a 50-Ω system. Because power is fed through standard 50-Ω cables, the generator can be remotely located and can be quickly connected. It has a more stable frequency output since the matching system in the RF heater is automatically adjusted to maintain the load impedance at 50 Ω. The 50-Ω systems are more expensive than the open circuit ones, and have not been popularly used by industries. The open circuit RF system generates heat by means of an RF generator that produces oscillating fields of electromagnetic energy and comprises a powersupply and control circuitry, a parallel plate and a system for supporting processed material as described in Fig. 1. The target material placed between top and bottom electrodes is moved on a conveyor belt to simulate continuous processes, and acts as a capacitor to store electrical energy and a resistor to transfer electric energy to thermal energy. The top electrode plate with adjustable height is inductively coupled to the tank oscillator circuit via feed strips. The power supplied to the sandwiched object is typically controlled by varying the electrode gap in most industrial systems.

2.2. Mechanisms of RF heating

DPs influence reflection of electromagnetic waves at interfaces and the attenuation of the wave energy within materials (Birla et al., 2008b). That in turn determines the amount of energy absorbed and converted into heat. DPs related to RF heating are permeability, permittivity (capacitivity), and electrical conductivity of the heated material. It is generally accepted that, for most dielectric materials, permeability has no or very small contribution to dielectric heating, and so it is usually not considered (Zhang and Datta, 2001). The permittivity that determines the dielectric constant (ε'), the dielectric loss factor (ε''), and the loss angle, influences the RF heating. The ε' and ε'', which are the real and imaginary parts of the complex permittivity, respectively, of ε, are given by:

$$\varepsilon = \varepsilon' - j\varepsilon'' \tag{1}$$

where ε is permittivity (F/m), ε' is often called the dielectric constant or "capacitivity", describing the degree of a material's interaction with an alternative electrical field, and quantifying its ability for reflecting, storing, and transmitting electromagnetic energy. ε'' is commonly called dielectric loss factor, which is a measure of the ability of a material to dissipate electrical energy into heat, and $j = (-1)^{0.5}$. A material with a low ε'' may absorb less energy and could be expected to heat poorly in an electrical field due to its greater transparency to electromagnetic energy (Marra et al., 2009).

In practice, the DPs of materials relative to that of vacuum are used. The relative permittivity (ε_r), relative complex permittivity ($\varepsilon_r^{'}$), and the relative loss factor ($\varepsilon_r^{''}$) are related as follows:

$$\varepsilon_r = \varepsilon / \varepsilon_0 = \varepsilon' / \varepsilon_0 - j\varepsilon'' / \varepsilon_0 = \varepsilon_r' - j\varepsilon_r'' \tag{2}$$

where ε_0 is the permittivity of electromagnetic wave in free space (8.854×10^{-12} F/m).

An important thermo-physical property that affects RF heating of foods is electrical conductivity (σ, S/m), which is defined as the ability of a food to conduct electric current. Electrical conductivity is related to the ionic depolarization that occurs within the food during RF heating. σ of a material can be expressed by the following equation (Piyasena et al., 2003):

$$\sigma = 2\pi f \varepsilon'' = 2\pi f \varepsilon_0 \varepsilon_r'' \tag{3}$$

where f is the electromagnetic frequency (Hz).

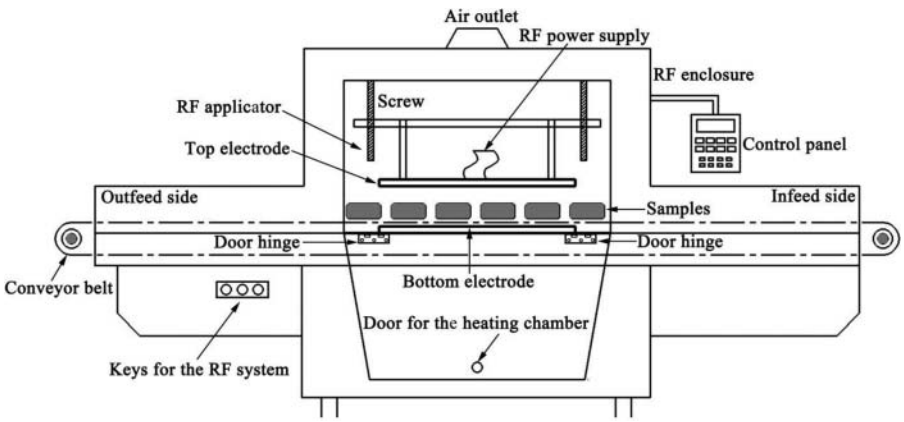

Figure 1. Schematic diagram of the radio frequency (6 kW, 27.12 MHz) heating system.

The tangent of the dielectric loss angle (tan δ) is often called the loss tangent or the dissipation (power) factor of the material. For a given material, this is equivalent to the ratio of ε'' over ε':

$$\tan\delta = \varepsilon'' / \varepsilon' = \varepsilon_r'' / \varepsilon_r' \quad (4)$$

The DPs of food products are affected by many factors, including frequency, temperature, and moisture content. The mechanisms that contribute to the dielectric loss in heterogeneous mixtures include dipole, electronic, atomic, and Maxwell–Wagner responses (Fig. 2). For moist dielectric materials, ionic conductivity plays a major role at lower frequencies (e.g.,<200 MHz), whereas both ionic conductivity and dipole rotation of free water play a combined role at MW frequencies. The Maxwell–Wagner polarization effect peaks at about 0.1 MHz, but in general, its contribution is small compared to that of ionic conductivity (Tang et al., 2005). For foods with low moisture content, dipole dispersion of free water molecules is negligible, so the bound water plays a major role in dielectric heating in the frequency range from 20 to 30,000 MHz. Bound water is a form of water that has its mobility between ice and free water. Bound water molecules have a lower relaxation frequency than free water at around 100 MHz (20°C), and the magnitude is also much smaller than free water. It could be found that both the bound water and Maxwell–Wagner's effects contribute to the DPs at a very low range comparing with free water and ionic effects. This explains the low values of DPs in low moisture foods.

From Fig. 2, we can see that the influence of ionic conduction is always positive when temperature increases. At the RF and MW frequency of practical importance and current applications in food processing (RF: 1 to 50 MHz and MW: 915 and 2450 MHz), ionic conduction and dipole rotation are dominant loss mechanisms (Ryynänen, 1995):

$$\varepsilon'' = \varepsilon_d'' + \varepsilon_{\sigma'}'' = \varepsilon_d'' + \frac{\sigma}{2\pi f \varepsilon_0} \quad (5)$$

where subscripts d and σ' stand for contributions due to dipole rotation and ionic conduction, respectively.

Penetration depth (d_p, m) of RF power is defined as the depth where the power is reduced to $1/e$ (e = 2.718), about 37%, of its value at the surface of the material. The d_p value in a lossy material can be calculated as follows (Marra et al., 2009):

$$d_p = \frac{c}{2\sqrt{2}\pi f\left[\varepsilon'\left(\sqrt{1+\left(\frac{\varepsilon''}{\varepsilon'}\right)^2}-1\right)\right]^{\frac{1}{2}}} \quad (6)$$

where c is the speed of light in free space (3×10^8 m/s). Due to the much longer wavelength (11 m at 27 MHz), RF energy penetrates further into food materials than MW (0.12 m at 2450 MHz). This factor is important in the selection of the appropriate thickness of a material bed to ensure a uniform heating during the RF process.

2.3. RF power density

An open circuit RF system consists of a high voltage transformer, a rectifier, an oscillator tube, a tuned circuit, an impedance coupling and matching circuit, and an applicator (Fig. 3). The line power from the wall is transformed to a high voltage, and converted into DC power by a rectifier. The oscillatortube excites high frequency alternating electromagnetic waves and transports them to the tank circuit to be tuned to a specific working frequency and to match the load. The applicator receives the high-frequency electromagnetic wave, and the load in it converts the electromagnetic wave into heat.

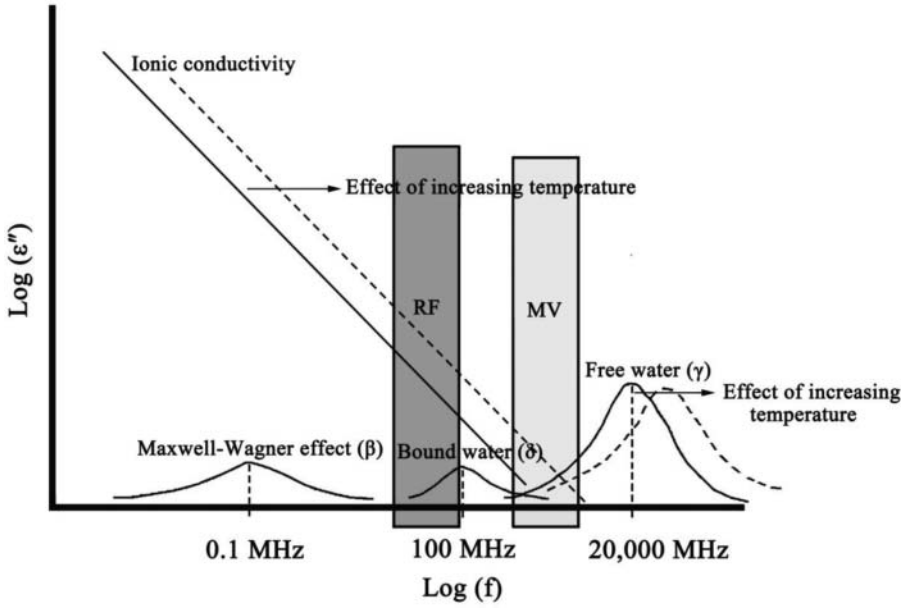

Figure 2. Contribution of various mechanisms to the loss factor of food materials as functions of frequency and temperature (Tang et al., 2002).

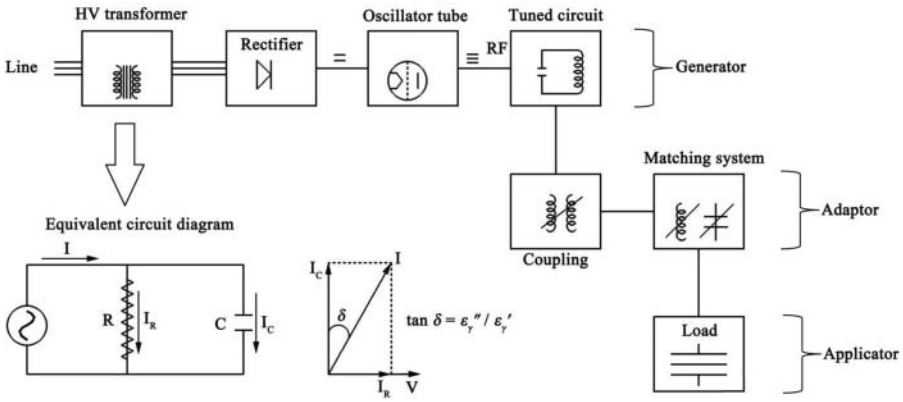

Figure 3. Scheme of a typical open circuit RF system (Zhao et al., 2000).

In principle, if there is a dielectric material between two electrodes, the material would become a resistance, and the current flowing through the resistance is in phase with the applied voltage. For the most commonly used flat capacitor, an AC displacement current passes throughout the food, the capacitance can be expressed as (Zhao et al., 2000):

$$C = \frac{\varepsilon_0 \varepsilon_r' A}{d} \tag{7}$$

where C is the capacitance (F), A is the area of an electrode (m^2), and d is the distance between the two electrodes (m).

Figure 3 shows the circuit diagram of a dielectric heating system and the current directions. The current through the capacitorcan be expressed by:

$$I_C = \omega V C = \omega V \varepsilon_0 \varepsilon_r' \frac{A}{d} \tag{8}$$

where I_C is the electric current (A),ω is angular frequency ($\omega = 2\pi f$, rad/s), and V is the electricpotential between the two electrodes (volt) and is related to the electrical field strength ($E = V/d$, volt/m). The current through the load (I_R) can be expressed by:

$$I_R = I_C \tan\delta = \omega V \varepsilon_0 \varepsilon_r' \frac{A}{d} \tan\delta = 2\pi f \,|\vec{E}\,|\, \varepsilon_0 \varepsilon_r'' A \tag{9}$$

The power dissipated in the load can be expressed by:

$$Q = I_R V = 2\pi f \,|\vec{E}\,|^2 \varepsilon_0 \varepsilon_r'' dA \tag{10}$$

where $|\vec{E}\,|$ is electric field strength (V/m) in the food load and dA is the volume of load. So the power dissipated per unit volume (P, W/m^3) can be rewritten as follows:

$$P = 2\pi f \,|\vec{E}\,|^2 \varepsilon_0 \varepsilon_r'' = 5.56 \times 10^{-11} f \varepsilon_r'' \,|\vec{E}\,|^2 \tag{11}$$

The electromagnetic field energy is converted into thermal energy through interactions with a dielectric material.

2.4. Electromagnetic field and Maxwell equation solutions

Modeling RF treatments in food processing applications involves the simulation of the electric and magnetic fields that pass throughout the food, and its interaction with food molecules and the simulation of heat transfer within the product. A brief theoretical explanation of what RF energy is and how it interacts with food matteris needed to understand their general behaviors. The general approach for solving electromagnetic field in 2-and 3-D requires the application of Maxwell equations in differential form (Neophytou and Metaxas, 1998):

$$\vec{\nabla} \times \vec{E} = \frac{\partial \vec{B}}{\partial t} = -\mu \frac{\partial \vec{H}}{\partial t} \tag{12}$$

$$\vec{\nabla} \times \vec{H} = \vec{J} + \frac{\partial \vec{D}}{\partial t} = \sigma_c \vec{E} + \varepsilon_0 (\varepsilon' + j\varepsilon'') \frac{\partial \vec{E}}{\partial t} \tag{13}$$

$$\vec{\nabla} \cdot \vec{D} = \vec{\nabla} \cdot \varepsilon \vec{E} = \rho_e \tag{14}$$

$$\vec{\nabla} \cdot \vec{B} = \vec{\nabla} \cdot \mu \vec{H} = 0 \tag{15}$$

where $\vec{E}$ is electric field intensity (V/m), $\vec{B}$ is magnetic flux density (Wb/m^2), $\vec{H}$ is magnetic field (A/m^2), $\vec{D}$ is electric flux density (C/m^2) of the dielectric material, μ is magnetic permeability (H/m), ρ_e is free volume charge density (C/m^3), $\vec{J}$ is the current density (A/m^2), and σ_c is electrical conductivity (S/m) of the material.

In problems of wave propagation, the behavior of an electromagnetic wave is concerned in a source-free region where ρ_e and J are zero. Equations (12)–(15) can be combined to give a second-order homogeneous vector wave equation in E and H alone.

$$\nabla^2 \vec{E} - \mu\varepsilon \frac{\partial^2 \vec{E}}{\partial t^2} = 0 \tag{16}$$

Field vectors that vary with space coordinates and are sinusoidal functions of time can similarly be represented by vector phasors that depend on space coordinates but not on time. The RF field can be seen as a time harmonic field, and the electric

field strength can be expressed below:

$$\vec{E}(x,y,z,t) = \mathrm{Re}[\vec{E}(x,y,z)e^{j\omega t}] \quad (17)$$

where $\mathrm{Re}[E(x,y,z)e^{j\omega t}]$ is the real part of $[E(x,y,z)e^{j\omega t}]$, and t is the time period (s). When the time harmonic assumption is made, Eqs. (12)–(15) become:

$$\vec{\nabla} \times \vec{E} = -j\mu\omega\vec{H} \quad (18)$$

$$\vec{\nabla} \times \vec{H} = j\varepsilon_0\varepsilon_r\omega\vec{E} \quad (19)$$

Under time harmonic condition, the effect of the magnetic field is negligible, Eq. (18) can be ignored and Eq. (19) can be changed to:

$$\vec{\nabla} \times \vec{H} = (\sigma + j\omega\varepsilon)\vec{E} = j\omega\left(\varepsilon^* + \frac{\sigma}{j\omega}\right)\vec{E} = j\omega\varepsilon_c\vec{E} = \vec{J} \quad (20)$$

In existing RF applicators, the wavelength in the RF range is often much larger than the maximum size of the object to be heated, quasi-static approximation can be applied for the solution of Maxwell's electromagnetic field equations. Since the scalar voltage potential (V) is related to electric field by $\vec{E} = -\vec{\nabla} V$, and current density $\vec{\nabla} \cdot \vec{J} = 0$, Eq. (20) can also be modified to Laplace equation (Metaxas, 1996):

$$-\vec{\nabla} \cdot ((\sigma + j2\pi f\varepsilon_0\varepsilon')\vec{\nabla} V) = 0 \quad (21)$$

The electric field at any point inside the electrodes is governed by Eq. (21). In this case, as boundary conditions, the top electrode is set as the electromagnetic source since it introduces the high frequency electromagnetic energy and the bottom electrode is set as ground conditions ($V = 0$). RF applicator walls are electrically insulated, so last boundary conditions are:

$$\vec{\nabla} \cdot \vec{E} = 0 \quad (22)$$

The analytical solution of La place equation for the electric potential between RF electrodes and heat dissipation in a slab sandwiched between electrodes can be coupled together, and an expression for electric potential on upper electrode can be obtained as (Birla et al., 2008a):

$$V = \left(d_{air}\sqrt{(\varepsilon')^2 + (\varepsilon'')^2} + d_{mat}\right)\left(\sqrt{\frac{\rho c_p}{\pi f\varepsilon_0\varepsilon''}\frac{dT}{dt}}\right) \quad (23)$$

where d_{air} is the air gap between top electrode and food sample (m), and d_{mat} is the height of the food material (m). The electrode voltage would change as a function of spatial location between the two electrodes.

2.5. Heat transfer modeling

The common objective in modeling RF heating is to obtain the temperature profile inside the food. The equations representing the electromagnetic and the thermal phenomena must be solved inside the food itself. Once electromagnetic model has been solved, heat generation can be derived from electromagnetic fields and material properties. Therefore, a link has to be created between the electromagneticequations and heat transfer equations. The amount of power (P, W/m^3) converted from electromagnetic energy to thermal energy is related to the DPs of treated materials. For a given electric field intensity ($|\vec{E}|$, V/m), P was already introduced above (Eq. (11)), as described below (Choi and Konrad, 1991):

$$P = 2\pi f\varepsilon_0\varepsilon''|\vec{E}|^2 = \omega\,\varepsilon_0\varepsilon''|\vec{E}|^2 \quad (24)$$

where $|\vec{E}|$ is the modulus of the E-field, that—in case of RF heating—can be evaluated in accordance with the La place equation (Eq. (21)), stated for electroquasi-static conduction in inhomogeneous materials. Here, volumetric energy generation term depends on the electric fieldsexperienced within the food, the frequency of electromagnetic field, and DPs of the material to be heated.

The mathematical description of heat transfer within the food product placed between the electrodes, is given by unsteady heat-conduction equation (assuming that a solid-like foodstuff is processed in the RF applicator) with a generation term, coupled with the quasi-static electro-magnetic field equations:

$$\rho c_p\frac{\partial T}{\partial t} = \vec{\nabla} k \cdot \vec{\nabla} T + P \quad (25)$$

where ρ is density (kg/m^3), c_p is specific heat (J/kgK), k is thermal conductivity (W/m K), T is the temperature (K), and t is the time (s). While the solution of heat transfer is needed just within the sample, the Gauss law must be evaluated for the space between the two electrodes, which includes the sample and the air around it (Marra et al., 2007).

It must be emphasized that in the whole RF systems (i.e., the RF applicator plus the food sample undergoing RF heating) the displacement of the electromagnetic field is needed (as described by Eq. (21)), while in the food sample the coupling with the heat transfer equation is strictly needed (as described by Eqs. (24) and (25)). This concept is summarized in the

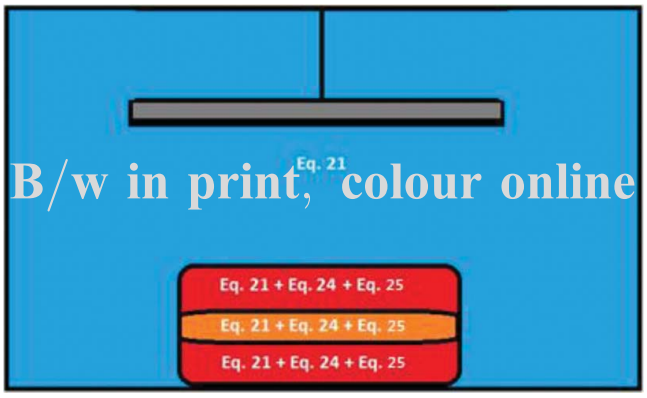

Figure 4. Sketch of a RF heating systems, with a food product constituted by two substrates (red and orange color regions) surrounded by air (blue region), and reference to modeling equations applying in the different regions.

following Fig. 4, where—as an example—the case of RF heating of a food product constituted by two components is sketched, together with the reference to the equations needed to mathematically describe the RF heating of the considered food product. It is clear from this sketch that, while solving the set of equations, one has to take into account the physical (density, specific heat, and thermal conductivity) and the dielectric (dielectric constant and loss factor) properties of the material in which that equation is considered. In this way, it is possible to model the selective RF heating, since different substrates may heat faster or slower depending on their different loss factors. The same concept applies when the goal is to study the effect of RF heating on insects in host products (such as fruits). When the applied frequency and electric fields are the same both for the pests and the host products, the heat produced in the insects and the host products might be different, resulting in the different final temperatures of the insects and the host products after the same period of RF heating (Huang et al., 2015a).

For the heat transfer equation to determine the temperature distribution inside the food undergoing RF heating, initial and boundary conditions are needed. A uniform temperature T_0 can be assumed within the food sampleas initial condition. On boundary conditions, convective heat transfer from the external surfaces, in accordance with the Newton lawformulated as follows:

$$-k\cdot\vec{\nabla}T\cdot\vec{n} = h\,(T-T_{air}). \tag{26}$$

where h is the overall external convective heat transfer coefficient (W/m^{2}K), T_{air} is the air temperature inside the RF cavity (K) and$\vec{n}$ is the normal vector of the surface.

Moisture transfer can occur during many heating operations whena certain amount of the energy being transferred to the food sample. The amount of thermal energy required to change the state of water (that is contained in the food) from liquid to vapor at a given saturation temperature and pressure is called the latent heat of evaporation. Under such condition, the latent heat of evaporation must be supplied. The internal vapor pressure caused by evaporation of the liquid water is generated quickly, and this pressure is possibly the main driving force behind moisture transfer into vapor and/or liquid forms. The vapor pressure of a liquid increases with increasing temperature. The molecules in the liquid are more energetic at higher temperatures, and more molecules can escape from the liquid phase into the gas phase. A pressure of 20 kPa and a temperature of 60°C correspond to the "liquid-vapor" separate region. Therefore, the driving force of the moisture transfer from the sample to the surrounding air starts to be important when processes characterized by temperatures above 60°C (it means that the vapour pressure is higher than 20 kPa) for long time. In operations conducted below 60°C and for short processing times, in a first mathematical model formulation of RF heating, the moisture transfer and its effect on the heat transfer can be ignored.

When the moisture transfer from the sample to the surrounding aircannot be ignored, the thermal effects of evaporation must be taken into account at least at the boundaries between the sample and the surrounding air. On these surfaces, the internal conduction is balanced by the external convective heat transfer and by the heat loss due to the evaporation of moisture, as in the following expression (Marra et al., 2007):

$$-k\,\vec{\nabla}T\cdot\vec{n}\;|_{\,boundary\,-} = [h(T-T_{air})+\dot{m}_w\lambda]\,|_{\,boundary\,+} \tag{27}$$

where $\dot{m}_w$ is the amount of water evaporated per unit of time- and surface area (kg/m^2 s) and λ is the latent heat of vaporisationper unit mass of evaporated water (J/kg).

Of course, the amount of water evaporated per unit of time- and surface area ($\dot{m}_w$) could be computed by adding another equation that describes the mass transfer at the boundary between the food sample and the surrounding air:

$$\dot{m}_w = k_m\,(c_{ws}-c_{wair}) \tag{28}$$

where c_{ws} and c_{wair} are the mass concentration of water (kg/m^3) at the food external surface and in the air far from the food sample, respectively and k_m (m/s) represents a coefficient of convective mass transfer.

A finer modeling approach would also require coupling the mass transfer (Dhall and Datta, 2011; Pace et al., 2011; Zhu et al., 2015), thus adding another partial differential equation in a porous-media (Datta et al., 2007; Ni et al., 1999) or conjugate approach (Marra et al., 2010).

2.6. Computer simulation of RF heating in food processing

Activities of computer simulation fall into two general categories, the first being the simulation of heat transfer within the product (load) between the electrodes and focusing mainly on the description of transport phenomena inside the food. The second area has been modeling RF heating in terms its electric and magnetic fields. Table 1 gives a summary of recent development of computer simulation for RF heating in food processing and postharvest treatments. It can be seen from literatures that the computer simulation could be used to understand the mechanisms, test new strategies, optimize parameters, and design appropriate RF treatment conditions for specific food products.

2.6.1. Computer simulation of RF heating and drying

The first attempt to model RF systems was reported in the 1990s (Baginski et al., 1989, 1990). These efforts attempted to model the electromagnetic and thermodynamic phenomena for industrial-scale RF drying chambers. Subsequently, Neophytou and Metaxas (1996, 1997, 1998, 1999) recommended that solution of Laplace equation is adequate for small-sized applicators, whereas wave equations should be used for large size electrodes. This opened opportunity for analyzing the electromagnetic field distribution, heating rate, and heating pattern in foods with FEM during RF heating. The application of a three-dimensional (3D) finite-element computer program package, TLM-FOODHEATING, on the simulation of capacitive RF dielectric heating ofradish and alfalfa seeds was investigated by Yang et al.

Table 1. Summary of computer simulation for RF heating in food processing and post-harvest treatments.

Purpose	Food Items	Software	Technique	Temperaturedependent properties	Dimension	Affiliation	References
Insect control	Almonds	VisualBasic	FEM	–	–	Northwest A&F University, China	Wang et al. (2013)
	Apple	FEMLAB 3.2	FEM	√	3D	Washington State University, USA	Birla et al. (2008a)
	Avocado	FEMLAB 3.4	FEM	√	3D	Washington State University, USA	Birla et al. (2008b)
	Dry soybeans	COMSOL 4.3a	FEM	√	3D	Northwest A&F University, China	Huang et al. (2015a, c)
	Dried nuts	VisualBasic	FEM	–	–	Washington State University, USA	Wang et al. (2003a)
	Grapefruit	FEMLAB 3.4	FEM	√	3D	Washington State University, USA	Birla et al. (2008b)
	In-shell walnuts	VisualBasic	–	–	–	Washington State University, USA	Wang et al. (2005)
	Mung beans	COMSOL 4.3a	FEM	√	3D	Northwest A&F University, China	Huang et al. (2015b)
	Orange	FEMLAB 3.4	FEM	√	3D	Washington State University, USA	Birla et al. (2008b)
	Raisins	COMSOL 4.2a	FEM	√	3D	Washington State University, USA	Alfaifi et al. (2014)
	Stored-grain	MATLAB R2011a	–	–	–	University of Saskatchewan, Canada	Shrestha and Baik (2013)
	Wheat	COMSOL 4.3a	FEM	√	3D	Northwest A&F University, China	Chen et al. (2016)
	Wheat flour,	FEMLAB 3.4	FEM	√	3D	Washington State University, USA	Tiwari et al. (2011b)
	Wheat kernels	COMSOL 4.2	FEM	√	3D	Shanghai Jiao Tong University, China	Jiao et al. (2015a)
Pasteurization or sterilization	In-shell eggs	COMSOL 3.4	FEM	–	3D	McGill University, Canada	Dev et al. (2012)
	Peanut butter	COMSOL 4.2a	FEM	–	3D	Washington State University, USA	Jiao et al. (2014a, 2015b)
	Shell eggs	COMSOL 4.3a	FEM	√	3D	University of Nebraska – Lincoln, USA	Lau et al.(2016)
	Soybean flour	COMSOL 4.3a	FEM	√	3D	Northwest A&F University, China	Huang et al. (2016a)
	Wheat	COMSOL 4.3a	FEM	√	3D	Northwest A&F University, China	Chen et al. (2015b)
Temperature and electrical field analyses	Alfalfa and radish seeds	TLM-FOOD HEATING	Finite different time domain method	√	2D-axi	University of Connecticut, USA	Yang et al. (2003)
	1% of CMC powder	HFSS	FEM	√	3D	Washington State University, USA	Chan et al. (2004)
	Meat batters	FEMLAB 3.1	FEM	√	3D	Università degli studi di Salerno, Italy	Marra et al. (2007)
	Meat batter	COMSOL 3.5	FEM	√	3D	Università degli studi di Salerno, Italy	Uyar et al. (2014)
	Meat batter	COMSOL 4.3b	FEM	√	3D	Università degli studi di Salerno, Italy	Uyar et al. (2016)
	Raw potato	FAM	FEM	–	2D-axi	University of Cambridge, UK	Neophytou and Metaxas (1996, 1997, 1998, 1999)
	Salt solution	C++	–	√	–	Washington State University, USA	Jiao et al. (2014b)
Thawing	Lean beef	COMSOL 4.3b	FEM	√	3D	Università degli studi di Salerno, Italy	Uyar et al. (2015)
	Mashed potato	COMSOL 3.2a	FEM	√	3D	Washington State University, USA	Wang et al. (2008a)
	Tuna	FEMAP, PHOTO-Wave-jω and Photo-Thermo software	FEM	√	3D	Tokyo University of Marine Science and Technology, Japan	Llave et al. (2015)

(2003). They successfully solved the EM field by the transmission line method and the heat diffusion by the standard explicit finite difference time domain method. Chan et al. (2004) developed an effective model to simulate an actual RF heating cavity using the wave equation applied in 3D instead of the conventional electrostatic method. Similarly, Jumah (2005) solved the partial differential equations for modeling the RF-assisted fluidized bed drying of grains.

The temperature profiles and the nonuniformity of temperature distribution occurring during RF heating of cylindrical meat batters, were analyzed by mathematical modeling of both electromagnetic and thermal phenomena (Marra et al., 2007). The goodness of model fit was evaluated by comparing numerical results with measured temperature profiles. Multiphysics phenomena during RF heating of a foodstuff, shaped as cube, cylinder, or sphere, have been theoretically studied by Romano and Marra (2008). Tiwari et al. (2011a) employed a finite element model to explore the effects of sample size, shape, position, and dielectric properties of wheat flour and the surrounding medium, electrode gap, and top electrode configuration on the RF power uniformity in wheat flour placed into a 12 kW, 27.12 MHz parallel plate RF system and showed that these factors significantly affected the RF power distribution in RF-treated flour. Then, a sensitivity study indicated that the heating uniformity of the raisins was most affected by the density of the samples followed by the top electrode voltage, the DPs, the thermal conductivity and the heat transfer coefficient (Alfaifi et al., 2014). Simulation results also demonstrated that the variation in sample density and specific heat, especially thermal conductivity, had a relatively slight effect on RF heating rate (Huang et al., 2015b). The RF heating rate was significantly influenced by electrode gap, top electrode voltage, and the DPs and moisture content of the sample (Jiao et al., 2014b).

Huang et al. (2015c) developed a computer simulation model using a finite element-based commercial software and validated it using experimental dry soybeans packed in a rectangular container ($300 \times 220 \times 60$ mm^3) and heated in a 6 kW, 27.12 MHz RF system. The experimental results were in good agreement with the simulation ones, and both showed higher temperature values in the middle and bottom layers compared with those of the top layers. Corners and edges were heated more than center areas in all layers. Therefore, rounding the edges and corners in the containers or bending the top and bottom electrodes was key methods to control the electrical field inside the RF system (Alfaifi et al., 2016; Huang et al., 2016b). More recently, Uyar et al. (2016) developed a numerical model to analyze power absorption, temperature distribution, heating rates and heating uniformity in processed food material during RF heating when different projection areas and different distances between electrodes were considered. Results showed that geometrical factors, such as the projection of sample exposed surfaceon electrode surface and the distance between electrodes, have a significant influence on heating rate, heating uniformity and power absorption in block-shaped foods undergoing RF heating.

2.6.2. Computer simulation of RF pasteurization and sterilization

In the specific application of RF energy to food sterilization processes, both simulation and experiment results confirmed that the hot spots were located at the places near the corner of the sample (mashed potato), and the cold spots were at the center of the sample (Wang et al., 2008a). The temperature differences between the simulation and experiment at cold spots were within 5% (i.e., 6°C at 120°C), which limited the sterilization value (F_0) error to 3 min. During the food sterilization process, due to the exponential nature of the sterilization calculation, a small difference at temperatures above 121°C can introduce a large variation in sterilization value. For example, an 11% temperature difference at 121°C represents a 13°C temperature difference between experiment and simulation, which would cause a significant error in predicting the F_0 by simulation results. To guarantee the safety of commercially sterilized food, it is necessary to assure that the F_0 of the cold spot reaches the designated value.

According to the recommendations of USDA-FSIS for the pasteurization of eggs, egg white must be heated up to 57.5°C, and the egg yolk has to be heated up to 61.1°C for 2 min (Dev et al., 2012). For the individual whole eggs, which heated with RF heating in a vertical alignment in air would form a coagulation ring at the interface between the albumen, air cell, and shell before the yolk was sufficiently pasteurized. This phenomenon was caused by redirection and concentration of the electric field in the shell-air cell-albumen interface due to starkly different dielectric properties (Lau et al., 2016). Maxwell's equations and Fourier's equation were solved for obtainingthe temperature distribution in eggs and the locations of hot and cold spots were determined (Dev et al., 2012). Their results showed that egg white gets heated up faster than the egg yolk in the parallel plate RF applicator, which was not desirable to sustain the functional properties of the egg. When the individual whole eggs were rotated between the electrodes, the egg yolk was heated more than the egg white as preferred. For the egg products in packages, it was possible to achieve more heating of the yolk than the white when the eggs were kept static and heated in the coaxial cavity RF applicator (Dev et al., 2012). This set up would be suitable for applications at an industrial scale. Therefore, two types of RF applicators namely parallel plate RF applicator and coaxial cavity design were simulated and it was found that both the processes would be suitable for in-shell pasteurization of eggs.

Commercial peanut butter in a cylindrical jar was used as a model of low moisture food subjected to RF heating when the cold spot location reached the target pasteurizing temperature (70°C) in a 6 kW, 27.12 MHz RF system. Based on both experiment and simulation results, the cold spot location was found to be at the center of top and bottom surfaces for samples with or without PEI sheets. Their results indicated that the use of the PEI addition method has improved heating uniformity by reducing themaximum temperature differencefrom 28 to 18°C in the peanut butter and therefore enhanced the potential for pasteurization of low moisture foods heated in RF systems. After that, Jiao et al. (2015b) showed that a pair of PEI blocks with a diameter of 8 cm among all five diameters (2, 4, 6, 8, and 10 cm) added to the cold spots of a given peanut butter sample could

make the sample reach the best heating uniformity. Furthermore, the best height of PEI blocks with a diameter of 8 cm that allows the sample to be heated most uniformly was found to be 1.3 cm after sweeping from 0.1 to 2.3 cm with a step of 0.1 cm.

2.6.3. Computer simulation of RF disinfestations

Differential heating or selective heating is a main advantage of RF heating as compared to the conventional and MW heating for disinfestations. To provide a theoretical basis and experimental evidence to support the hypothesis that insect larvae can be preferentially heated in food products by RF heating for pest control. Wang et al. (2003a) developed a mathematical model based on heat transfer and dielectric heating to predict preferential heating of insect pests in dry nuts. The model results showed that the temperature of insects is 14.3 ± 1.1°C higher after 4 min of RF heating at 27 MHz than that of the walnut kernels. The heating rate for the insect slurry is 1.4–1.7 times faster than for walnut kernels, confirming that the insects are indeed preferentially heated in walnuts. Therefore, when the applied frequency and intensity of the electric fields are the same both for the pests and the host products, the heat produced in the insects and the host products might be different due to different loss factor, resulting in different final temperatures of the insects and the host products after the same period of RF heating (Huang et al., 2015a). To examine the relative electric field intensities in the insects (E_i) and the host products (E_p), a theoretical model was developed on the basis of interaction of electromagnetic waves with multi-phase materials as following (Shrestha and Baik, 2013):

$$E_i = E_p\left(\frac{3\varepsilon_p}{2\varepsilon_p + \varepsilon_i}\right) \tag{29}$$

where ε_i is the relative complex permittivity of the insect (F/m), ε_p is the relative complex permittivity of host products (F/m), E_i is the electric field within insect bodies (V/m), and E_p is the electric field within host products (V/m).

To analyze the electric field distribution of insects under different conditions, Eq. (29) can be shown as:

$$E_{ip} = \frac{E_i}{E_p} = 3\left(\frac{1}{2 + \varepsilon_i / \varepsilon_p}\right) \tag{30}$$

where E_{ip} is the ratio of E-fields per unit volume in the insect relative to that in host medium.

To investigate the feasibility of RF selective heating of insect larvae in soybeans, Huang et al. (2015a) solved the coupled electromagnetic and heat transfer equations for developing a simulation model. Simulated and experimental results both showed that cold spots were located at the center part of each layer. After 6 min RF heating, the mean temperature differences between insects and soybeans at the top, middle, and bottom layers were 5.9, 6.6, and 6.2°C, respectively. Their results revealed that the heating rate of insects was 1.4 times greater than that of soybeans. The simulated selective heating of insects in soybeans may provide potential benefits in developing practical RF treatments to ensure reliable control of insect pests without adverse effects on product quality.

2.6.4. Computer simulation of RF thawing

The coupled electro-thermal problem of modeling an RF process becomes more complicated for simulation of thawing since the phase change process requires dealing with evolving large latent heat over a small range of temperature. Llave et al. (2015) constructed a 3D geometric model using FEMAP, the boundary and loading conditions, electric intensity, and other parameters used in the model were set in Photo-Wave-jω for analysis of the electromagnetic field, and set in Photo-Thermo for the heat transfer analysis to estimate the temperature distribution. To validate the simulated results, the tuna samples were thawed from −60 to −3°C (center temperature) using a 13.56 MHz parallel plate RF system and by thawing in air. The validated model was then successfully applied to studying the effects of electrode size on temperature uniformity in the RF thawing of frozen tuna muscle.

Uyar et al. (2015) also developed a computational modelin a 3D domain with temperature-dependent thermo-physical properties (TPs) and DPs to improve the heating uniformity and to minimize runaway heating in a 50-Ω and a free running oscillator RF system. The boxed frozen lean beef sample (≈3.84 kg), shaped as a parallelepiped (200 × 200 × 100 mm^3) was placed in a polypropylene container (not immersed in water) on the center of the bottom electrode during RF experiments. Nonuniform temperature distribution during thawing, especially high temperatures encountered along the surface and corners of the product, is a major disadvantage of a RF thawing system. As demonstrated by Uyar et al. (2015), during defrosting, thawing of outer surfaces occurs at the initial stages, while still frozen inside as parts are being surrounded by a low thermal conductivity layer leading to longer thawing times. Therefore, the thawing times are always higher for the larger sizes, and this issue makes the RF processes an unavailable industrial process. Therefore, it is necessary to systematically study the RF thawing characteristics and evaluate treatment parameters toimprove the RF thawing uniformity in food industry based onthe validated computer model.

3. Computer simulation for evaluating RF heating uniformity in food processing

3.1. The nonuniform RF heating characteristics

The sheer number of research on using RF heating in food applications gives a wealth of information for understanding the process better (Fu, 2004; Hou et al., 2016; Marra et al., 2009; Piyasena et al., 2003). However, wide temperature variations were observed within heated samples during RF heating of different kinds of fruits (Alfaifi et al., 2014), grains (Jiao et al., 2015a), meat (Llave et al., 2015; Zhang et al., 2004), model foods (Birla et al., 2008a), ready-to-eat meals (Orsat et al., 2001), vegetables (Liu et al., 2015), and various agricultural products (Fu, 2004; Gao et al., 2010). Moisture accumulationat the surface of food during RF heating was studied by Datta and Ni (2002). The temperature difference between the hottest and the coldest spots in mashed potatoes (295 × 235 × 42 mm^3) was greater than 30°C, after 320 s of RF heating (Wang et al., 2008a). Cold and hot spots occur in food load during dielectric heating due to nonuniform electrical field distribution.

Temperature variation over the cross section of apple was distinct with contour of maximum temperature (80°C) at fruit core and minimum temperature (55°C) at surface from the simulation results (Birla et al., 2008b). Both simulated and experimental results showedthat immersion of the centerplaced model fruit in waterslightly shifted the hot spot toward the core of the modelfruit. Moreover, the presence of water radically enhanced power coupling as it took only half time (7 min) what required for RF heating of the fruits in air to reach ~50°C temperature. Under similar conditions, very high electric field concentrations occurred at the corners and edges of the cube, edges and the middle of the cylinder, whereas maximum *E*-field was at the bottom of the sphere (Birla et al., 2008a). Tiwari et al. (2011b) reported that nonuniform temperature distribution may cause quality loss due to over or underheating in different parts of a food product. Nonuniform temperature distribution resulting in cold spot has serious concerns in meat products because of the survival of the bacteria resulting in health hazards (Rincon et al., 2015).

A 3D finite element model of heat transfer in food material during RF heating was developed by Alfaifi et al. (2014). Experiments were conducted using raisins as test material packed in a rectangular plastic container (25.5 × 15.0 × 10.0 cm^3). Both results showed thatthe temperatures were highest in the middle layer (45–76°C), whereas they were lower in the top and the bottom layers (41–62°C and 40–57°C). Overheating was observed at the edges and corners of the top (51 and 62°C), middle (65 and 76°C), and bottom (48 and 57°C) layers (Fig. 5). According to Alfaifi et al. (2014), overheating behavior at the edge and corners could be attributed to the refraction and reflection of the electric field at interfaces, resulting in a higher volumetric power density at these positions. The temperature distribution patterns were similar to those reported by Tiwari et al. (2011b) and Huang et al. (2015c).

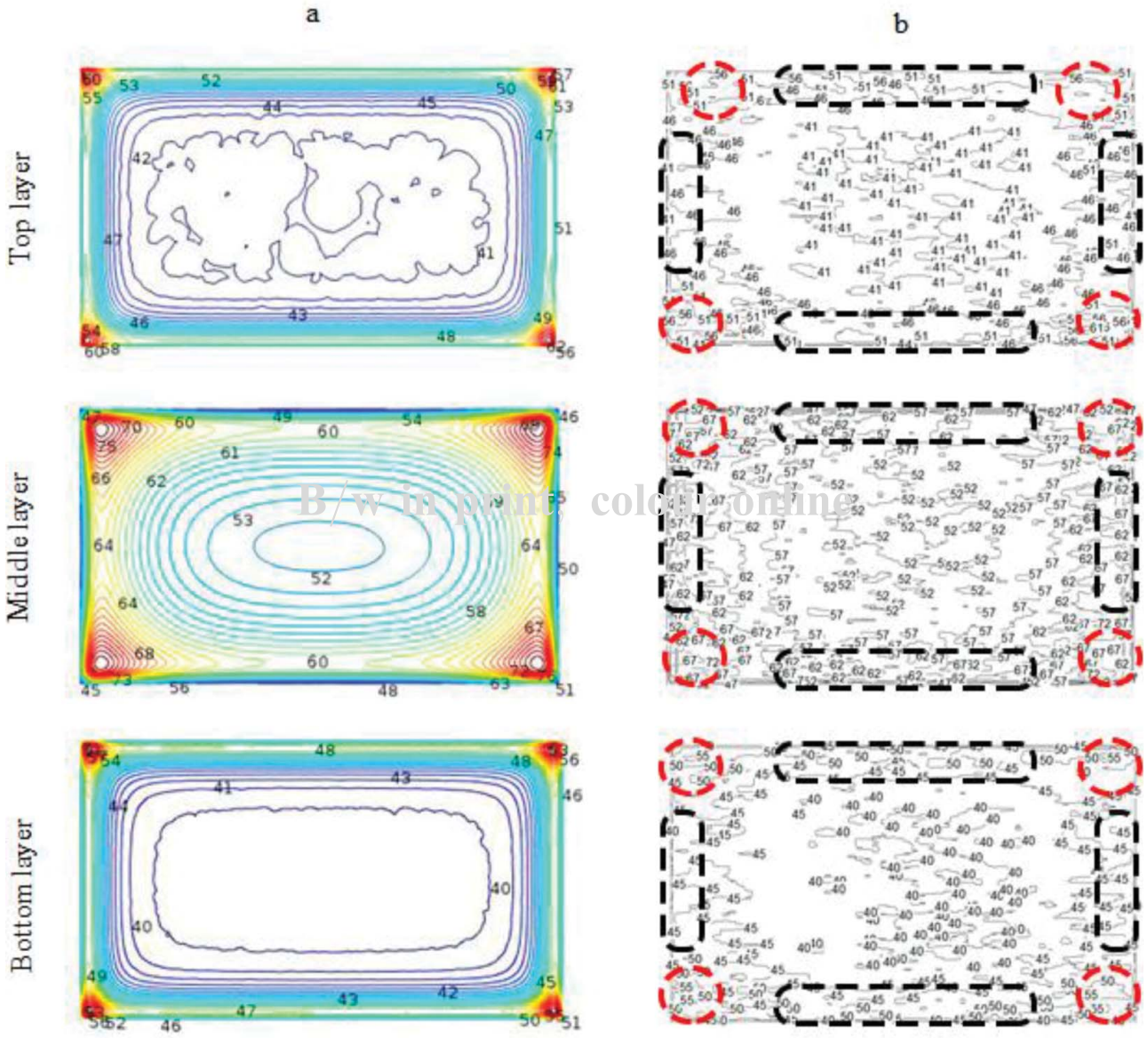

Figure 5. Simulated (a) and experimental (b) temperature distributions of top, middle, and bottom layers of raisin samples placed in a polypropylene container (255×150×100 mm^3)in the center and middle between the top and bottom electrodes of the RF system after 4 min heating at a fixed electrode gap of 13.6 cm and initialtemperature 23°C (Alfaifi et al., 2014).

Tiwari et al. (2011b) claimed that the temperature values were higher at the middle layers and temperature at the top surface was lower than that in the middle layer because of a large evaporation at the top surface. It is clear from the literature that with the help of simulations, it may be possible to find new ways to overcome nonuniform RF heating and speed up the incorporation of RF heating in the food industry with acceptable heating uniformity and product quality.

3.2. Thermo-physical and dielectric properties of food products

To model the RF heating process, it is necessary to know the DPs and TPs of the food material. A review of DPs and TPs measurement techniques was given by Venkatesh and Raghavan (2005). DPs and TPs data for foodstuffs used in computer simulationat RF frequencies over the range of treatment temperatureswere taken from the literature and summarized in Table 2.

3.2.1. For pulverized or solid foods

For pulverized or bulk materials, the overall volume of samples was simplified as a whole in the simulation model, which ignoring the influence of air gap between the food samples. DPs and TPs of food products were assumed to be homogeneous and isotropic, the density was assumed as temperature independent and other properties were temperature dependent. It should be noted that this method is complementary to ensure good model accuracy and maintain convergent simulation results. A considerable amount of work on DPsof food and agricultural products has been published at RF frequencies (Hou et al., 2016; Nelson, 2008; Piyasena et al., 2003). These data were subjected to linear regression analysis for using these properties in simulation model over the treatment temperatures range (Alfaifi et al., 2014).

For some solid foods, due to the fact that phase change in some food substances occurs during RF thawing over a range of temperature and large latent heat evolves over this range, special techniques were required to deal with such problems (Pham, 2006). Liu et al. (1999) reported the possible techniques to determine the specific heat, density, and thermal conductivity of food products by the following equations:

$$\rho = \left\{ \begin{array}{cc} \rho_1, & T \geq T_{sh} \\ \rho_e + S_d(T_{sh} - T) + (\rho_1 - \rho_e)\dfrac{(T_{sw} - T_{sh})}{(T_{sw} - T)}, & T < T_{sh} \end{array} \right\} \tag{31}$$

$$c_p = \left\{ \begin{array}{cc} c_1, & T \geq T_{sh} \\ c_e + \dfrac{D}{(T_{sw} - T)^n}, & T < T_{sh} \end{array} \right\} \tag{32}$$

$$k = \left\{ \begin{array}{cc} k_1, & T \geq T_{sh} \\ k = k_e + S_k(T_{sh} - T) + (k_1 - k_e)\dfrac{(T_{sw} - T_{sh})}{(T_{sw} - T)}, & T < T_{sh} \end{array} \right\} \tag{33}$$

where T_{sw} is the normal freezing temperature for pure water (K), T_{sh} is the initial freezing point of the food (K), S_d is the changes in density per unit change in temperature (kg/m^{3}K), S_k is the changes in thermal conductivity per unit change in temperature (W/mK^2), ρ_e (kg/m^3), c_e (J/kgK), k_e (W/mK), D (J/K^{n}kg), and n are the empirical constants in Eqs. (31), (32), (33), (32) and (32), respectively.

3.2.2. For granular and porous foods

Both granular and porous foods are two-media systems composed of air and solids. Air has different DPs values from thoseof a solid food, and a change in bulk density may lead to a change in the DPs of food. The higher the bulk density, the higher the dielectric constant and loss factor observed, which means more amount of mass interacting with the electromagnetic fields (Nelson and Trabelsi, 2012). This is especially important for particulate materials and porous-packed samples. It is difficult to directly measure the bulk DPs and TPs for such materials (Içier and Baysal, 2004a, b). Nelson (2008) proposed several dielectric mixture equations to calculate the DPs of air particle mixtures. The Landau and Lifshitz, Looyenga equation (LLLE) is described as (Liu et al., 2009):

$$\varepsilon^{\frac{1}{3}} = v_a(\varepsilon_a)^{\frac{1}{3}} + v_s(\varepsilon_s)^{\frac{1}{3}} \tag{34}$$

where ε is the complex permittivity of the mixture, ε_a is the complex permittivity of the air, ε_s is the complex permittivity of solid, v_a is the volume fraction of the air, and v_s is the volume fractions of particles, where $v_a + v_s = 1$. Dielectric mixture equations have been used successfully to predict the DPs of various bulk materials that consist of air voids and solid particles (Kim et al., 1998; Liu et al., 2009). The calculated DPs of bulk materials were reduced as compared to these properties at particle density (0% air) due to the presence of air (Alfaifi et al., 2014; Jiao et al., 2015a).

The Kopelman model mixture equation was used to estimate the thermal conductivity for granular and porous foods (Alfaifi et al., 2014):

$$k_e = k_s\left(\frac{1 - v_a^{2/3}(1 - (k_a / k_s))}{1 - v_a^{2/3}(1 - (k_a / k_s))(1 - v_a^{2/3})}\right) \tag{35}$$

where k_e is the effective thermal conductivity for the bulk mass (W/m°C), k_s and k_a are the thermal conductivity of solid and air (W/m°C), and v_a is the volume fraction of the air. This equation has been successfully used to determine the thermal conductivity of tortilla chips (Moreira et al., 1995) with an error range of ±4.3–9.1%, and that of French fries (Sahin et al., 1999) with an error range of ±2.5–8.3%.

3.3. Criterion to evaluate RF heating uniformity

The well-developed simulation model makes it possible to obtain convergent results from various agricultural products. Different criteria and indexes have been used to study, evaluate, and compare the RF heating uniformity in food products. The uniformity of temperature distribution in an RF processed sample is a significant parameter and especially affected by the absorbed power of the sample. Analysis of the quantity of the absorbed power by the sample during a RF heating process was

Table 2. DPs and TPs of various food products and materials used in mathematical modeling.

Product	Process conditionT- (°C)	Dielectric constant	Loss factor	Specific heat (J/kg°C)	Thermal conductivity (W/m°C)	Density (kg/m^3)	Electrical voltage (V)	Reference
Albumen	T=20–70	$0.0053T^2$-$0.45T$+ 90.67	$205.6T^{0.465}$- 326.7	$6.53\times10^{-6}T^3$ $-7.87\times10^{-4}T^2$ $+2.14\times10^{-2}T$+3.42	$2.50\times10^{-6}T^2$ + $3.63\times10^{-4}T$ + 0.54	1045	8000	Lau et al. (2016)
Apple (green)	T=20–60	$-0.152T + 75.7$	$2.857T + 60.2$	3700	0.422	790	–	Birla et al.(2008b)
Apple (red)	T=20–60	$-0.196T + 78.52$	$2.179T + 45.68$	3600	0.513	840	–	Birla et al. (2008b)
Avocado	T=20–60	$0.63T + 104.36$	$14.47T + 393.94$	3380	0.42	1060	9500	Birla et al. (2008b)
Beef meats	T=-18-(+10)	$-18\leq T<$-10:-$0.108T^2$-$1.91T$+19.75 -10$\leq T\leq$1:0.699T^2+12.33T+81.21 1$<T\leq$10:-0.189T^2+2.437T+72.37	$-18\leq T<$-10:-$1.08T^2$+$0.09T$+61.75 -10$\leq T\leq$-1:3.647T^2+62.15T+307.15 -1$<T\leq$10:-0.112T^2+7.092T+255.73	$T\leq T_{m1}$: 1935.2 $T_{m1}\leq T\leq T_{m2}$:153016.3 $T>T_{m2}$:3497.4	0.47–0.152	$T<T_{m1}$: 961 $T_{m1}\leq T\leq T_{m2}$: 1007 $T>T_{m2}$: 1053	141.42	Uyar et al. (2015)
Butter	T=20–60	2.3	1.0	2720	0.29	911	–	Chen (2015a)
Cherry	T=20–60	$-0.046T + 92.44$	$6.836T + 159.2$	3643	0.511	1010	–	Birla et al. (2008b)
Cheese	T= 20–80	$54.6 + 0.28T$	$160.6 + 11.2T$	3700	0.48	1013.2	–	Wang et al. (2012)
Gellan gel	T=20–60	$-0.21T + 86.76$	$4.36T + 129.4$	4160	0.53	1010	9500	Birla et al. (2008b)
Grapefruit	T=20–60	$0.17T + 85$	$5.01T + 95.21$	3703	0.54	950	9500	Birla et al. (2008b)
Lean tuna	T= −20-(+10)	$-20\leq T<$-5:0.06T^2+2.62T+31.5 -5$\leq T\leq$1:-11.364T^2-2.454T+291.64 1$<T\leq$10:-2.23T+278.56	$-20\leq T<$-5:0.338T^2+10.886T+84.65 -5$\leq T\leq$1:-20.42T^2-2.026T+540.55 1$<T\leq$10:-4.23T+524.93	$T\geq T_{sh}$:3650 $T<T_{sh}$:c_p=1179 +173900/$(T_{sw}$-$T)^{-1.628}$	$T\geq T_{sh}$:0.523 $T<T_{sh}$:k=k_e+0.01518(-1-T)+ (k_1-k_e)·(T_{sw}+1)/(T_{sw}-T)	1070	–	Llave et al. (2015)
Mashedpotato	T= 20–80	83.3–0.14T	173.2–16.4T	3763	0.548	1000	–	Chen et al. (2013); Wang et al. (2008a)
Meat batters	T= 20–80	0.0011 T^2- 0.5531T + 109.43	$-0.0058\ T^3 + 5.32\ T^2 - 1609.1\ T +$ 161643	3600	0.01088T-0.0848	1057	173.21	Marra et al. (2007); Uyar et al. (2016); Romano and Marra (2008)
Meatballs	T= 20–80	$62.6 + 0.29T$	$198.4 + 12.6T$	3600	0.48	1144.7	–	Wang et al. (2012)
Mung beans	T=20–60	$0.021T + 1.82$	$0.0028T + 0.036$	$18T + 1165$	0.102	953	8400	Huang et al. (2015b)
Noodles	T= 20–80	98.9–0.34T +2×$10^{-3}T^2$	$203.1 + 13.0T$	3690	0.52	977	–	Wang et al. (2012)
Orange (pulp)	T=20–60	$-0.22T + 88.6$	$4.9T + 122.6$	3661	0.580	1030	9500	Birla et al. (2008b)
Orange (peel)	T=20–60	$3.94T + 58.2$	$-0.16T + 82.53$	3300	0.40	800	9500	Birla et al. (2008b)
Pasta	T=20–60	46.0	15.4	2460	0.50	1050	–	Chen et al. (2015a)
Peanut butter	T=20–80	4.03	0.4	2030	0.209	1115	12,100	Jiao et al. (2014a, 2015b)
Polystyrene	T=20	2.6	0.0003	1300	0.036	25	–	Huang et al. (2016b)
Polypropylene	T=20	2.0	0.0023	1800	0.2	900	–	Alfaifi et al. (2014)
Polyetherimide	T=20	3.15	0.0025	2000	0.122	1270	–	Jiao et al. (2014a)

Potato	T= 20–70	50	15	3900	0.4	1000	–	Geedipalli et al. (2007)
Raisins	T=20–60	$0.08T + 6.3$	$0.02T + 1.9$	$10.9T + 1831$	$0.001T + 0.15$	784	4100	Alfaifi et al. (2014)
Sauce	T= 20–80	$101.8–0.932T + 1.16\times10^{-2}T^2$-$4\times10^{-5}T^3$	$418.3 + 25.9T$	3730	0.51	905.6	–	Wang et al. (2012)
Sauce	T=20–60	69.4	25.2	3000	0.50	1050	–	Chen et al. (2015a)
Shell	T=20–70	$3.081T^{0.3072} + 4.45$	$216.9T^{0.04521}$- 236.8	$8.52\times10^{-7}T^3$-$1.30\times10^{-4}T^2$ $+8.64\times10^{-3}T+0.90$	$8.50\times10^{-5}T^2 - 1.03\times10^{-3}T +$ 0.68	2300	8000	Lau et al. (2016)
Soybeans	T=20–80	3.6	0.26	1737	0.11	748	5000	Huang et al. (2015c)
Soybean flour	T=20–60	3.96	0.38	$5.8T + 1614$	$0.0007T + 0.083$	380	4050	Huang et al. (2016a)
Tap water	T=20–60	$-0.48T + 84.74$	$0.33T + 11.1$	4180	0.56	1000	9500	Birla et al. (2008b)
Walnut	T= 20–60	$0.01T + 4.7$	$0.0003\ T^2 - 0.0289T + 1.08$	2510	–	900	–	Wang et al. (2003a)
Whey protein gelb	T=20–60	$0.28T + 93.56$	$17.51T + 468.23$	3850	0.55	1050	9500	Chen et al.(2013)
Wheat	T=20–60	4.30	0.11	2670	0.15	860	15,000	Chen et al. (2015b)
Wheat kernels	T=20–80	$0.002T^2$-$0.16T$+5.097	$0.001T^2$−$0.091T$+1.695	$13.158T$+1537.4	$0.0031T$+0.0506	803	5100	Jiao et al.(2015a)
Wheat flour	T=20–70	$0.00077T^2$-$0.0345T$+3.72	0.33	$23T + 757$	$1.36\times10^{-4}T^2$-$0.0094T + 0.2819$	800	13,000	Tiwari et al. (2011b)
Yolk	T=20–70	$12.82T^{0.1975} + 28.24$	$278.4T^{0.2599}$- 431.9	$4.12\times10^{-6}T^3$-$5.75\times10^{-4}T^2$ $+2.37\times10^{-2}T$+2.50	$1.07\times10^{-6}T^2 + 1.41\times10^{-4}T +$ 0.35	1148	8000	Lau et al. (2016)

conducted by Neophytou and Metaxas (1998). Tiwari et al. (2011a) defined the power uniformity index (PUI) where the smaller PUI value demonstrates an improved power uniformity in the processed sample, and a well-designed RF system was reported to result in lower PUI values:

$$PUI = \frac{\frac{1}{V_{vol}}\int_{V_{vol}} sqrt((Q - Q_{av})^2) dV_{vol}}{Q_{av}} \quad (36)$$

where the minimum value of PUI is zero, which indicates uniform RF power in dielectric materials.

The average RF power density (Q_{av}, W/m^3) in a dielectric material is defined as the volume integral of the RF power density (Q, W/m^3) divided by material volume (V_{vol}, m^3).

$$Q_{av} = \frac{1}{V_{vol}}\int_{V_{vol}} Q dV_{vol} \quad (37)$$

Besides the changes in the processed and absorbed powers, temperature-related calculations were other approaches to determine the temperature distribution uniformity in the treated products. The heating uniformity of the treated samples was evaluated using the heating uniformity index (λ). It is defined as the ratio of the rise in standard deviation of sample temperature to the rise in average sample temperature during treatment and can be calculated by the following equation (Wang et al., 2005):

$$\lambda = \frac{\Delta\sigma}{\Delta\mu} = \frac{\sqrt{\sigma^2 - \sigma_0^2}}{\mu - \mu_0} \quad (38)$$

where σ_0 and σ are the standard deviations of the initial and final temperature distributions, respectively. μ_0 and μ are the means of the initial and final temperature distributions, respectively. The smaller the λ value, the better the RF heating uniformity. Heating uniformity index was used for evaluating RF heating uniformity in almond (Gao et al., 2010), corn (Zheng et al., 2016), coffee bean (Pan et al., 2012), legumes (Jiao et al., 2012; Wang et al., 2010), rice (Zhou and Wang, 2016), and walnut (Wang et al., 2007a).

Another formulation of a temperature uniformity index (UI) of the treated samples in simulation is given by the following equation (Alfaifi et al., 2014):

$$UI = \frac{\frac{1}{V_{vol}}\int_{V_{vol}} \sqrt{(T - T_{av})^2} dV_{vol}}{T_{av} - T_{initial}} \quad (39)$$

where V_{vol} is the material volume (m^3), T and T_{av} are local and average temperatures (K) inside the dielectric material over the volume (V_{vol}, m^3). This index is a useful tool to evaluate the heating uniformity when using a fixed configuration and a specific RF unit. The smaller UI values indicate an improvedRF heating uniformity.

A new temperature uniformity index (TUI) was proposed based on Alfaifi's UI by replacing the average temperature (T_{av}) with the target temperature (T_t) in the following form (Jiao et al., 2015b):

$$TUI = \frac{\int_{V_{vol}} | T - T_t | dV_{vol}}{(T_t - T_{initial}) V_{vol}} \quad (40)$$

where T_t is the target heating temperature (K). Also in this case, a smaller index corresponds to better heating uniformity. The new TUI might be more suitable for describing the heating uniformity of a pasteurization/sterilization process, which requires the cold spot location to reach a certain target temperature needed for controlling pathogens. It would reflect the degree to which temperature in the volume deviated from the target temperature.

3.4. Factors influencing RF heating uniformity

During RF processing, several interacting factors influence heating uniformity. These factors include the design of RF heating systems (e.g. the inductance positions and feeding strips, electrode shape and electrode configuration), packaging geometries, DPs, and TPs of the treated materials, position of the treated materials within the RF units, and the surrounding media (Fu, 2004). The following subsection summarizes various factors that influence RF heating uniformity.

3.4.1. Nonuniformity due to electromagnetic field

The nonuniform electromagnetic field distribution is the major factor resulting in nonuniform heating during RF treatments (Wang et al., 2007a). Many factors are included in the design of RF heating systems, such as the voltage of the top electrode, electrode shape, and power output, shape, TPs and DPs of the samples, and position of the samples in the RF units, which may influence electromagnetic field distributions in RF-treated agricultural products (Fu, 2004; Marra et al., 2009; Tiwari et al., 2011a).

The electric field between two parallel plate electrodes was in parallel lines uniformly spaced throughout the region between two electrodes, and perpendicular to their surfaces with no dielectric material placed in it (Huang et al., 2016a). Fig. 6 shows a typical electromagnetic field distribution for a rectangular-shaped dielectric material placed between two parallel plate electrodes. When the dielectric material was placed at the center of the bottom electrode with an air gap over it, the presence of the surrounding air causes an intensification of the heating near the top of the electrode space at the edges of the material, forming hot spots and cold spots. Samples placed in the middle of RF electrodes showed higher electricfield intensity at their central section as electric field deflected by both (top and bottom) edges with increased electricfield concentration at the central parts of the sample (Uyar et al., 2015). Therefore, it is essential that the electromagnetic field within food geometry should be uniform to ensure even heating. To achieve this, some additional methods (electrode attachments, sample movement, and/or mixing) could be used to ensure RF heating uniformity in industrial applications. According to Alfaifi et al. (2016) and Huang et al. (2016b), the uniformity of electromagnetic field for a rectangular shaped food sample was improved

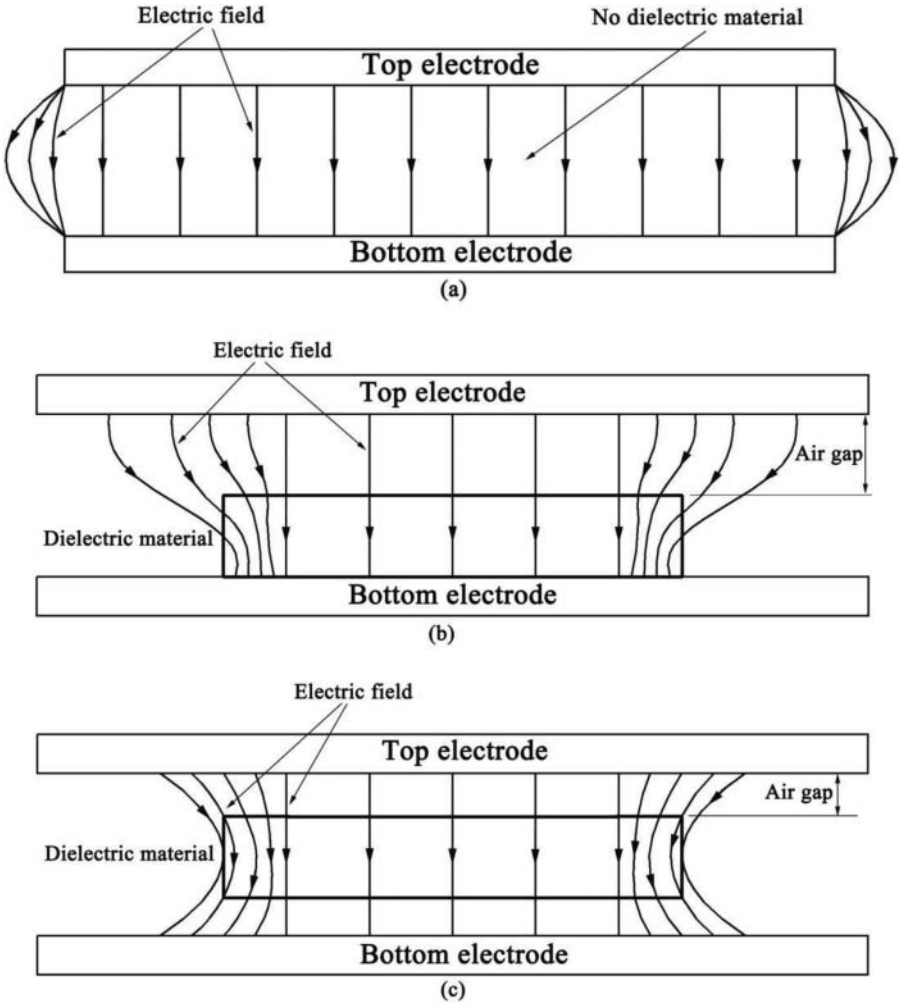

Figure 6. The electric field strength between two parallel plate electrodes with (a) no dielectric sample, (b) dielectric sample placed on the center of bottom electrode, (c) and dielectric sample placed in the center and middle between top and bottom electrodes (Huang et al., 2016a).

by rounding corners and reducing edges of the package geometry, and modifying electrode configurations.

3.4.2. Nonuniformity due to RF power and top electrode voltage

Marra et al. (2007) studied temperature distributions in cylindrical meat batters during RF treatments at different output powers and heating rates by solving the electromagnetic and heat equations using the finite element analysis. The authors reported that using lower output power resulted in more even temperature distributions. On the other hand, Romano and Marra (2008), by a mathematical model for simulation of RF heating using meat batter as the sample food, reported that the higher the applied power, the more uneven the temperature distribution. Based on vertical temperature measurements, the temperature gradient across the 1% CMC solutions was larger than that observed in tap water due to RF power decay, suggesting that more uniform heating can be achieved in low loss factor materials than that in high loss factor materials (Wang et al., 2008b). Their results also showed that the voltage of the top electrode is an important factor to influence the electromagnetic field intensity and final temperature distributions in samples. Huang et al. (2015b) reported that a higher top electrode voltage resulted in faster RF heating in mung beans during 6 min RF heating. With the important effect on RF heating rates, it is essential to precisely determine the top electrode voltage by direct measurement (Zhu et al., 2014).

3.4.3. Nonuniformity due to electrode configuration

The effect of the top electrode bending and angleson RF heating uniformity of samples was evaluated by Tiwari et al. (2011a). Results demonstrated that the top electrode bending position greatly affected the sample PUIas magnitudes of the electric fields and their distributions inside the sample changed with the top electrode bending positions and angles. Optimum RF power uniformity in a particular sample size could be achieved with a particular top electrode bending position and angle (Tiwari et al., 2011a). The effect of different combinations of the setback distances (distancebetween the edge of the sample and the bottom base and the topof the new designed electrodes)and bend angles on the heating uniformity of raisins packed in a rectangular-shaped container after RF heating to a central temperature of 52°C was explored by Alfaifi et al. (2016). These configurations were applied to both the top and bottom electrodes, and were attached to the flat top and bottom electrodes. They reported that treating materials with different

DPs, TPs and different container dimensions may require different electrode configurations. Besides, Wang et al. (2008b) also reported that the asymmetric connections of the inductor and the power supply to the top electrode resulted in an uneven standing wave pattern across the applicator. Therefore, a new symmetric design was developed by installing four conductors at the four corners on the top electrode and moved the feed strip to the center. The four corner inductors allowed independent adjustment of the voltage at each corner.

3.4.4. Nonuniformity due to electrode geometry and position

During RF processing, geometrical factors, such as distance between electrodes and projection of top electrode on the samples' exposed surface area (area that electric field passes through the sample) have a certain effect on heating uniformity in the samples (Uyar et al., 2016). Effect of the size of the projection of the top electrode on temperature distributions of tuna after RF thawing was evaluated by Llave et al. (2014). They reported that a more uniform temperature distribution was found with an electrode of the same size as the sample. The electrode size larger than the upper surface of the sample resulted in higher temperatures at the edges of the sample and the use of an electrode of smaller size than the sample showed an irregular temperature distribution (Llave et al., 2015). Huang et al. (2015c) also reported that when the top plate area was changed to 1.32 times of the sample size, the electric field started entering normally into the sample, and thus the hot spot in corners and edges of sample would be largely reduced.

According to Tiwari et al. (2011a), a proportion of oblique electric field, which caused the RF power nonuniformity, decreased when the electrode gap was reduced. However, an extremely reduced air gap might lead to runaway heating, which takes place when the warmest part of the product gets more power compared to colder parts due to higher rates of absorption. Uyar et al. (2014) showed that increased air gap between electrodes and sample surfaces with decreasing volume led the deflection of electric field to reduce its concentration inside the sample. Due to the significant effect of air gap as indicated above, when load sizes got smaller with the increase in the air gap, a major part of the electric field passed through the ground electrode without absorption by the sample. Therefore, Jiao et al. (2014b) corroborated the fact that the RF heating rate decreased as the electrode gap increased. For a fixed sample height, the air gap increases and the heating rate decreases with an increasing electrode gap (Huang et al., 2015b). When the air gap is reduced to zero, the value of ε' does not influence the heating rate. As a result, ε'' is the dominating factor in RF heating, and the heating mechanism changes from dielectric heating to resistive heating (Metaxas, 1996).

3.4.5. Nonuniformity due to food geometry and position

Effects of load shape, orientation, and position on the heating patterns during RF treatments were also investigated by Romano and Marra (2008). Among the sample shapes investigated by the authors, regular cubes were found to be more suitable for RF treatment since cubic-shaped products exhibited a fast and more uniform heating, with a good absorption of power (Tiwari et al., 2011a; Uyar et al., 2014). In case of cylindrically shaped products, authors recommended a vertical orientation during treatment, since horizontally oriented cylinders showed a slower heating, characterized by uneven temperature distribution (Wang et al., 2006b). Eventually, spherical shapes were found to be the less favored to RF heating (Birla et al., 2008a).

Simulated results conducted by Tiwari et al. (2011a) in dry food materials showed that the RF power uniformity should be better for sample sizes, either approaching zero or approaching the maximum possible size that can be kept completely between the RF electrodes. When sizes approached to zero, the major part of the electric field passed directly through the ground electrode, without entering into samples. With increase in sizes, most of the electric field entered obliquely as sizes were comparatively smaller than those of the upper electrode size (Jiao et al., 2015a). Oblique electric field increased the RF power nonuniformities in samples (Birla et al., 2008a). With a further increase in sample size, the electric field started entering normally (except a small area, which was getting deflected by sample edges and corners) into the sample (Marra et al., 2007). This caused increase in the RF power uniformity again. As demonstrated by Uyar et al. (2014), while the load volume changes from 100 to 1%, volume of air gap between electrodes and top-bottom surfaces of the sample increased. The smaller the load volume, the larger the air gap and the slower the heating rate. In a fixed air gap between electrodes and sample, the smaller the sample volume, the faster the heating rate of the sample. So that smaller volumes demonstrated higher temperature increase. According to Uyar et al. (2016), the effect of a decreasing sample volume was demonstrated to have a negative effect on the temperature evaluation if the electrodes were maintained at a constant distance. As a result, the wider projection area and shorter distance between electrodes led to faster heating, in terms of average temperature, but less uniform temperature distribution. The temperature distribution should be more uniform when samples were placed in the middle of RF electrodes as electric field deflected by top and bottom edges increased net electric field concentration at the central part of samples (Huang et al., 2015c; Jiao et al., 2015a; Marra et al., 2007). Similar results have been obtained by Birla et al. (2008a) and Tiwari et al. (2011a) when the small size sample was placed in the middle of RF electrodes, and the power uniformity would be clearly improved.

3.4.6. Nonuniformity due to food DPs and TPs

During RF heating, two physical factors, temperature and electric field intensity, interrelate with each other. In particular, the dissipated energy provided by electric fields heats those materials with temperature-dependent DPs. The variation, caused by temperature change and heat transfer, influences the electromagnetic field distribution. Hence, TPs and DPs of the product are the key factors to influence the uniformity of temperature distribution. Romano and Marra (2008) reported that the loss tangent first increased and then decreased with the increase in temperature of luncheon roll batter. Increasing the loss tangent, the dielectric absorption increases with the power absorbed within the domain. Wang et al. (2008a) also showed that the decreased electric field intensity caused by the increased loss

factor not only compensated for the influences brought by the increase in loss factor, but also influenced by the thickness of mashed potato and circulating water and their DPs and electric conductivity, respectively.

Birla et al. (2008b) demonstrated that increasing the ε'' value of the model fruit resulted in increasing heating rate only to a certain value. This was contrary to a general belief that increasing loss factor constantly increases heating rate inside the fruit. Beyond that value, increasing loss factor reduced the heating rate inside the fruit. Similar results demonstrated that a loss factor equal to the dielectric constant provided fast RF heating (Huang et al., 2015b; Jiao et al., 2014b). Rapid heating rates correspond to higher throughputs but may adversely affect the heating uniformity. Therefore, the differences in DPs and TPs among the components in a food may cause differential heating and thus temperature nonuniformity (Jiao et al., 2015b; Nelson, 2008). This may bring about a food safety issue for pasteurization and sterilization applications, and attention must be paid to find the cold spot(s) and make sure enough heating and lethality are achieved there (Jiao et al., 2014a). Huang et al. (2015c) corroborated the fact that the higher moisture contents along with the larger DPs and thermal conductivity, resulting in poor RF heating uniformity. Thus, dry products should provide a better uniform RF heating because of the smaller DPs (Tiwari et al., 2011a) as compared to high moisture food.

3.4.7. Nonuniformity due to properties of the surrounding medium

Birla et al. (2008a) reported that the nonuniform temperature distribution in fresh fruit subjected to RF heatingwas caused by the different DPs of food and the surrounding medium (usually air), which results in an unevenly distributed electric field. It has been reported that altering the DPs of water by addition of salt minimizes the differential heating between the fruit and water (Birla et al., 2008a). Therefore, Wang et al. (2008a) conducted a study for pre-packaged mashed potatoes heated in RF systems with circulating water to remove the heat accumulation at the edges. Water with various electrical conductivities was tested for heating rate, and the highest electrical conductivity (220 S/m) can reduce the hot and cold spot temperature difference from 30.9 to 24.2°C, and 22.4 to 13.6°C on different mashed potato samples. When the electrical conductivity of surrounding water increases, water should absorb most energy and food must be absorbing less energy, this could explain why the heating uniformity was improved. Tiwari et al. (2011a) reported that the PUI was the lowest when the surrounding material dielectric constant (between 8 and 11) was approaching to the dielectric constant value of wheat flour (fixed as 8). Theoretically, the dielectric constant determines the electric field distribution when the loss factor is far smaller than the dielectric constant (Metaxas, 1996).

The maximum temperature difference in the peanut butter was reduced from 28 to 18°C after using PEIassisting method, which has the closest dielectric constant (3.15) to that of peanut butter (4.03) and a lower dielectric loss factor (0.0025) (Jiao et al., 2014a). Huang et al. (2015c) also showed that the temperature uniformity could be achieved when the surrounding material dielectric constant (3) was approaching to the soybean samples (3.6). After that, Huang et al. (2016b) demonstrated that the heating uniformity was greatly improved by placing soybean samples in a polystyrene container, which had the closest dielectric constant (2.6) to that of soybeans (average value of 2.5 and 2.7 with moisture contents of 4.64 and 7.86% w.b.) and a lower dielectric loss factor value (0.0003). Therefore, the electric field distortion could be reduced by using a surrounding material with a low loss factor and a similar dielectric constant, instead of air (Huang et al., 2015c; Jiao et al., 2014a; Tiwari et al., 2011a). On the other hand, the container material, thickness, and corner radius were found to have a significant effect on heating uniformity of soybeans during RF processes (Huang et al., 2016b).

3.5. Solutions proposed for overcoming nonuniform RF heating

With the help of computer simulations, there have been various methods developed, accidental or on purpose, for various food products to improve the uniformity of RF heating (Table 3). The results of the various studies for various types of food materials, such asagricultural products (Huang et al., 2016b; Jiao et al., 2015a), fresh fruits (Birla et al., 2008a; Wang et al., 2006a), low moisture foods (Alfaifi et al., 2016; Chen et al., 2016), meat and fish (Llave et al., 2015; Uyar et al., 2016) to overcoming nonuniform RF heating are discussed in this section.

3.5.1. For meats and seafood

A number of researches have been conducted for overcoming nonuniform RF heating of meats and seafood, such as modifying electrodes, making the size of sample similar to that of the top electrode, and placing the sample in the middle of two electrodes. Most of the recent studies focused on the defrosting and thawing of meat and fish using RF heating, with successful results compared to those of conventional methods (Uyar et al., 2014). As described by Uyar et al. (2014), a cubic shaped luncheon roll meat was preferred as reference geometry for the load, as it exhibits a faster and more uniform heating with a good rate of power absorption (Romano and Marra, 2008). Therefore, a considerable number of food products are processed in rectangular boxes during RF heating. Uyar et al. (2014) confirmed that reducing electrode gap by increasing the load volume improved the RF power uniformity in the sample load. However, Llave et al. (2014) reported that greater uniformity of end-point temperature distribution of tuna muscle was obtained when the top electrode projection was similar in size to the sample, especially for samples with high-moisture content. In addition, greater uniformity of end-point temperature distribution was observed for low-fat content tuna muscle.

3.5.2. For fresh fruits and vegetables

For high water content food, like fresh fruits and vegetables, researchers used water surrounding combined with a moving or rotating method to enhance the RF heating uniformity. Birla et al. (2008a) reported that model fruit surrounded with air between RF electrodes and placed in the proximity of electrodes would not heat uniformly. Immersing the model fruit in water helped to reduce uneven heating within the model fruit. Therefore, they suggested that movement and rotation of the

Table 3. Simulation methods for overcoming nonuniform RF heating in the literature.

Method	Rationale	Food product	Reference
Surround the food with a cooling or heating medium	Reduces temperature variation in the food;	Apple	Birla et al. (2004)
		Bread	Liu et al. (2011, 2013)
		In-shell Macadamia nuts	Wang et al. (2014)
	Allows holding at a desired temperature	Lentil	Jiao et al. (2012)
		Orange	Birla et al.(2004)
		Roasted peanuts	Jiao et al. (2016)
		Walnut	Wang et al. (2007a)
Electrode modification	Reduce the fringe effect from the edges of the electrode	Fish	Llave et al. (2015)
		Raisins	Alfaifi et al. (2016)
		Soybeans	Huang et al. (2015c)
		Tuna muscle	Llave et al. (2014)
		Wheat flour	Tiwari et al. (2011a)
Intermittent stirrings and mixing	After mixing, the positions of the hot and cold spots mixed evenly; Temperature variations between central parts and corner and edge parts were reduced due to heatloss	Almonds	Gao et al. (2010)
		Chestnuts	Hou et al. (2014)
		Corn	Zheng et al.(2016)
		Pistachios	Ling et al. (2016)
		Rice	Zhou et al.(2015, 2016)
		Walnut	Wang et al. (2006b, 2007a)
		Wheat	Chen et al. (2015b)
Movement and rotation	Redistribute electric field and heat within the food product	Apple	Birla et al. (2004)
		Coffee bean	Pan et al. (2012)
		Eggs	Dev et al. (2012)
		Legume	Wang et al. (2010)
		Mango	Sosa-Morales et al. (2009)
		Orange	Birla et al. (2004)
		Walnut	Wang et al. (2005, 2007a)
		Wheat	Chen et al. (2016)
Placing in the middle of the electrodes	Avoids the electric field concentration at contact surfaces; Electric field deflected by top and bottom edges in the middle location	Dry soybeans	Huang et al. (2015c)
		Meat cubes	Uyar et al. (2014)
		Raisins	Alfaifi et al. (2014)
		Wheat kernels	Jiao et al. (2015a)
Using similar dielectric material around the samples	Reduces the disparity in DPs between the food and thesurrounding air, thus evening out the electric field distribution	Apple	Birla et al. (2004)
		Cherry	Ikediala et al. (2002)
		Cured ham	Bengtsson et al. (1970)
		Mango	Sosa-Morales et al. (2009)
		Mashed potato	Wang et al. (2008a)
		Orange	Birla et al.(2004)
		Peanut butter	Jiao et al. (2014a, 2015b)
		Scrambled egg	Luechapattanaporn et al. (2005)
		Soybean flour	Huang et al. (2016a)
		Stone fruit	Sisquella et al. (2013)

spherical object was the only plausible solution for improving heating uniformity. With rotation and movement of apples (Wang et al., 2006a), cherries (Ikediala et al., 2002), mangoes (Sosa-Morales et al., 2009), oranges (Birla et al., 2005), and persimmons (Tiwari et al., 2008) using a fruit mover, RF heating uniformity has been significantly improved. Finally, a saline water immersion technique or differential startup temperature should be adopted along with fruit movement and rotation during RF heating to minimize differential heating between fruit and water. As demonstrated by Wang et al. (2006a), preheating in hot water established a temperature gradient from the surface (44°C) to the core (36°C) and using preheated apples in RF-assisted heating treatments resulted in a fairly uniform temperature (47.3 ± 0.7°C) in fruit.

3.5.3. For liquid foods

To reduce fringe effect at the interface between the side of the food package and the air in the RF applicators, low conductivity water was used to immerse the food tray (with low conductivity too) to approximately match the DPs of the food. The water and package present a very flat surface to the imposed field, and push the boundary with air away from the food package. A pressurized vessel was developed to provide an overpressure of up to 0.276 MPa gauge (40 psig) that allows foods in large polymeric trays to be heated up to 135°C without bursting. The using of a pressure vessel in which a tray was immersed in circulating water enabled the heating of productsto 121°C utilizing RF energy (Wang et al., 2003b). The pilot-scale RF system operated at 27.12 MHz, 6 kW, and the pressure vessel was sandwiched between parallel electrodes (Wang et al., 2008a). The salt was added to closely match the sodium content of the packaged macaroni and cheese. With the assistance of circulating water at controlled temperatures, similar heating histories in model foods (20% whey protein gels, macaroni and cheese) were observed at different locations inside a tray. According to Wang et al. (2008a), the circulating water was pumped through the vessel before and during the heating process, which was used to improve the heating uniformity of mashed potato, including reduction of fringing electric field and edge-heating effects during the RF heating process.

3.5.4. For eggs and egg products

When the eggs were kept static and heated in parallel plate RF applicator, nonuniformity in heating led to accumulation of

cooked egg white at the top of the eggs (Dev et al., 2012). This was because the eggs were kept in a position where the heating took place from top to bottom in the parallel plate RF applicator. The nonuniformity in heating was convincingly reduced when the eggs were rotated between the electrodes. As the egg rotates, different region of the eggs were in close proximity to the electrodes at different times (Dev et al., 2012). Additional processing aids, such as cooling of the air cell, were recommended to ensure successful pasteurization of eggs using RF heating within a reasonable timeframe and with minimal quality issues (Lau et al., 2016). In addition, air bubbles could also be removed from food products using methods, such as ultrasonic treatment, to achieve better RF heating uniformity.

3.5.5. For low moisture foods

Several practical means can be used to minimize nonuniform RF heating in intermediate/low moisture foods, i.e. adding forced hot air to the product surface to increase the energy exchange between the product surface and surrounding air, sample movement and rotation or mixing during RF treatment (Birla et al., 2008a; Chen et al., 2015b, 2016; Tiwari et al., 2008). Wang et al. (2005) developed an intermittent stirring method during RF treatments to improve the heating uniformity for in-shell walnut. Their results showed a minimum of two stirrings were needed for desired uniformity and insect mortality. Tiwari et al. (2011a) confirmed that increasing electrode gap by reducing the load volume and the upper electrode bent to a certain angle improved the RF heating uniformity in the sample load.

The heating uniformity of RF-treated raisins were significantly improved when containers with rounded edges and corners were used, with a maximum temperature difference of about 12°C (Alfaifi et al., 2016). Using RF heating with a 2 cm set back distance and 90° angle of the newly designed electrodes, followed by forced hot air at 60°C improved the heating uniformity of the whole raisin samples with a temperature difference of about 5°C. Similarly, based on the heating uniformity studies for disinfesting chest nuts conducted by Hou et al. (2014), a RF treatment protocol was finally developed to combine 0.6 kW RF powers with a forced hot air at 55°C, movement of the conveyor, mixing twice, and holding at 55°C hot air for 5 min, followed by forced room air cooling through single-layer samples.

Subsequently, a simulation method of adding PEI cylindrical blocks on top of and at the bottom of peanut butter samples in a cylindrical jar has been evaluated, showing effective results to improve the RF heating uniformity (Jiao et al., 2015b). Their results revealed that the combination of PEI surrounding and the addition of 8 cm diameter PEI blocks could further reduce the temperature distribution range in peanut butter within 7.1°C when the peanut butter was heated from 23 to 70°C. Huang et al. (2016a) also demonstrated that the RF heating uniformity could be improved when the surrounding container dielectric constant was in a comparable range of the sample's, with the loss factor values of surrounding container lying between 0.01 and 0.1% of the sample's. Therefore, in practical applications for an industrial-scale RF system, which was equipped with an auxiliary hot air system and conveyor belt, choosing an optimum container material could be effectively minimize the effect of electric field bending and distortion within the corners and edges of food products during RF treatment.

3.5.6. For agricultural products

The heating uniformity of RF treated wheat samples was improved with the increasing mixing times based on experiment and simulation results (Chen et al., 2015b). Under mixing conditions, the maximum temperature of top layer in wheat sample reduced from 66.5°C to 51.0°C in experiment and from 68.3°C to 56.1°C in simulation after three time mixing during 3.5 min RF heating. Chen et al. (2015b) reported that in practical applications using several RF systems in series with mixings in between, forced hot air should be used to minimize the amount of heat loss during the mixing process. The same results have also been reported for stirring and mixing chestnut, lentil, soybean, walnuts, and wheat (Hou et al., 2014; Wang et al., 2007a, b; Wang et al., 2008c). Simulated results from Chen et al. (2016) demonstrated that moving and turning the container by 90° could improve the RF heating uniformity. During RF heating with three speeds of conveyor belt (v_1 = 8.57 m/h, v_2 = 14.23 m/h, and v_3 = 17.14 m/h) at a fixed gap of 120 mm, lower speeds of movement had a better heating uniformity. To get a better heating uniformity for agricultural products, they proposed to combine conveyor movement with adding forced hot air and mixing.

Moreover, according to the simulated results of Huang et al. (2015c), the RF heating uniformity of dry soybeans could be improved by using a suitable container material (with a similar dielectric constant to that of the sample), a smaller upper plate area (similar to the sample size), and placing the samples in the middle of two plate electrodes. In addition to this, the rectangular-shaped polystyrene container with rounded edges and corners (inner corner radius of 8 cm) combined with container thickness of 8 cm could provide good heating uniformity for soybeans (Huang et al., 2016b).

4. Suggestions for future research

Although continuous progress has been made in recent years in improving the accuracy of the modeling, much research work still needs to be carried out. The following section discusses the possible areas where further research could be performed to improve the accuracy of model prediction. More efforts are also needed to develop computer-aided engineering for a high degree of automation in industrial RF heating processes.

4.1. Surface heat and mass transfer coefficients

Heat and mass transfer coefficients are important parameters in modeling heating, drying, and cooling processes. The mass and momentum transfers of water within the food are commonly ignored due to a short RF heating time (< 5 min) and the influence on moisture content reduction is unnoticeable (< 2%) based on the reported research. For a long time RF heating (> 5 min) in high moisture content foods, three phases are considered in the treatment: solid (skeleton), liquid (water), and gas (water, vapor, and air). Based on the theory of mixtures (water, vapor, and air), the coupled electromagnetic and transport model needs to be developed for obtaining the moisture

content and mass fraction of vapor. Therefore, more reliable mathematical models need to be establishedby considering the heat and mass transfer coefficientsunder the given range of operating conditions.

4.2. Food properties and geometries

Food properties (DPs and TPs) are one of the most important factors determining the accuracy of model predictions. There is a critical need for the production of more DPs and TPs data on foodstuffs and potential packaging. This information is the key to improve understanding of temperature distribution but also is important in the design of RF heating systems. To simplify the model, bulk food products placed in the box or container is simplified as a whole in the simulation model. TPs and DPs of air particles mixtures are calculated by the dielectric and thermal mixture equations. This may be available for the small particle materials (almond, legume, peanut, raisin, and wheat kernel). But for the large particle products (apricot, date, fig, prune, and walnut) treated in RF systems, each single material should be constructedin a realistic geometric model. Thus, the computer program allows an independent and accurate simulation of solid-air interaction using a single particle approach.

4.3. Shrinkage and deformation during RF heating

Water in high moisture foods could be lost in an open package during the RF heating process. This water loss could result in an important size change that hinders the analysis of heat and mass transport and obtaining a convergent heating model. Shrinkage and deformation in foods occur due to moisture loss during thermal processes. Effects of shrinkage and deformation on the accuracy of RF heating models are sometimes significant. Therefore, both the water transport model and the mechanical deformation model should be taken into account in the future.

4.4. Coupling the heat and mass transfer model with other models

One of the critical roles of numerical modeling in the food industry is to analyze a heating process for producing a food product with high safety and quality. To obtain better understanding of the RF heating mechanism and improve the heating uniformity of various agricultural products in food industry, more attempts can be made to combine other models (biochemical reaction, microbial deactivation, and mechanics models) with the current heat and mass transfer models for further evaluating the safety and quality of foods during RF heating processes. Therefore, it is necessary to develop an advanced simulation model to simulate the industrial scale RF heating system, which combined the hot air-assisted RF heating with conveyor movement under mixing conditions.

4.5. Model library for various food products

There have been a number of publications in the area of computer simulation for the use of RF technology for food processing and preservation. Therefore, a simulation model library and the corresponding heat treatment process should be developed for various food materials processed in different conditions. When DPs and TPs of any kind of foods were entered to the model library, the best heat treatment protocol could be matched intelligently.

4.6. Computer-assisted design and automatic heat treatment process control

The application of numerical modeling of RF heating processes may benefit the understanding of the physics of a food processing operation and thus aid in design, optimization and control of a processing system. With a largestore and highspeed of models available in the food industry, more research should be stressed to practically use those models in design and control of a thermal processing system. The treatment parameter scan be controlled without delay by comparing 3D computer simulation results with the online real-time monitoring. The whole process of RF heat treatment can be realized automatically by using the computer control methods. The adjustment of the plate spacing, conveyor belt movement, and the application of the auxiliary measures (hot air) can all be changed automatically, which is applicable to industrial online production. Therefore, it is necessary to develop an advanced control system integrated with process optimization for a thermal process.

5. Conclusions

This paper has systematically reviewed recent developments in computer simulation for improving RF heating uniformity in the processed food. These methods include combination with an external heating or cooling device, enclosing in another medium, mixing or rotating food, modifying electrode shapes, and sample movement. Mathematical modeling improves the understanding of interaction of RF waves with food and is essential to the continued development of this novel technology. More research should be conducted to improve the accuracy of models by finding sufficientinformation on surface heat and mass transfer coefficients, food properties, and geometries during RF processing. More research should also be carried out on the heat and mass transfer through high moisture foods, deformation and shrinkage in RF heating processes. More efforts are also needed to establish a model library, couple the heat and mass transfer model with other models, and develop computer-aided engineering of RF processes on an industrial scale.

Acknowledgments

This research was conducted in the College of Mechanical and Electronic Engineering, Northwest A&F University. We acknowledge thefinancial support by research grants from General Program of National Natural Science Foundation of China (31371853) and Program of Introducing International Advanced Agricultural Science and Technologies (948 Program) of Ministry of Agriculture of China (2014-Z21). The authors thank Qian Hao, Xiaoxi Kou, Lixia Hou, Rui Li, Shuang Zhang, and Bo Zhang for their helps in collecting materials.

References

Alfaifi, B., Tang, J., Jiao, Y., Wang, S., Rasco, B., Jiao, S. and Sablani, S. (2014). Radio frequency disinfestation treatments for dried fruit: model development and validation. *J. Food Eng.* **120**:268–276.

Alfaifi, B., Tang, J., Rasco, B., Wang, S. and Sablani, S. (2016). Computer simulation analyses to improve radio frequency (RF) heating uniformity in dried fruits for insect control. *Innov. Food Sci. Emerg. Technol.* **37**:125–137

Awuah, G., Ramaswamy, H., Economides, A. and Mallikarjunan, K. (2005). Inactivation of *Escherichia coli K-12* and *Listeria innocua* in milk using radio frequency (RF) heating. *Innov. Food Sci. Emerg. Technol.* **6**:396–402.

Awuah, G. B., Koral, T. and Guan, D. (2014a). Radio-frequency baking and roasting of food products. **In**: *Radio-Frequency Heating in Food Processing: Principles and Applications*, pp. 231–243. George, B. A., Hosahalli, S. R. and Tang, J., Eds., CRC Press, Boca Raton, FL.

Awuah, G. B., Ramaswamy, H. S. and Tang, J. (2014b). Principles of radio frequency and microwave heating. In: *Radio-Frequency Heating in Food Processing: Principles and Applications*, pp. 3–20. George, B. A., Hosahalli, S. R. and Tang, J., Eds., CRC Press, Boca Raton, FL.

Baginski, M., Riggs, L., German, F. and Reed, M. (1989). Experimental and numerical characterization of the radio frequency drying of textile materials (I). J. Microw. Power EE. **24**:14–20.

Baginski, M., Broughton, R., Hall, D. and Christman, L. (1990). Experimental and numerical characterization of the radio frequency drying of textile materials (II). J. Microw. Power EE. **25**:104–113.

Bengtsson, N., Green, W. and Del, V. F. (1970). Radio-frequency pasteurization of cured hams. J. Food Sci. **35**:682–687.

Birla, S., Wang, S., Tang, J. and Hallman, G. (2004). Improving heating uniformity of fresh fruit in radio frequency treatments for pest control. Postharvest Biol. Technol. **33**:205–217.

Birla, S., Wang, S., Tang, J., Fellman, J., Mattinson, D. and Lurie, S. (2005). Quality of oranges as influenced by potential radio frequency heat treatments against Mediterranean fruit flies. Postharvest Biol. Technol. **38**:66–79.

Birla, S., Wang, S. and Tang, J. (2008a). Computer simulation of radio frequency heating of model fruit immersed in water. J. Food Eng. **84**:270–280.

Birla, S., Wang, S., Tang, J. and Tiwari, G. (2008b). Characterization of radio frequency heating of fresh fruits influenced by dielectric properties. J. Food Eng. **89**:390–398.

Brunton, N. P., Lyng, J. G., Li, W., Cronin, D. A., Morgan, D. and McKenna, B. (2005). Effect of radio frequency (RF) heating on the texture, colour and sensory properties of a comminuted pork meat product. Food Res. Int. **38**:337–344.

Chan, T., Tang, J. and Younce, F. (2004). 3-Dimensional numerical modeling of an industrial radio frequency heating system using finite elements. J. Microwave Power EE. **39**:87–105.

Chen, J., Pitchai, K., Birla, S., Gonzalez, R., Jones, D. and Subbiah, J. (2013). Temperature-dependent dielectric and thermal properties of whey protein gel and mashed potato. Trans. ASAE. **56**:1457–1467.

Chen, J., Pitchai, K., Birla, S., Jones, D., Subbiah, J. and Gonzalez, R. (2015a). Development of a multi-temperature calibration method for measuring dielectric properties of food. IEEE T. Dielect. El. In. **22**:626–634.

Chen, L., Wang, K., Li, W. and Wang, S. (2015b). A strategy to simulate radio frequency heating under mixing conditions. Comput. Electron. Agr. **118**:100–110.

Chen, L., Huang, Z., Wang, K., Li, W. and Wang, S. (2016). Simulation and validation of radio frequency heating with conveyor movement. J. Electromag. Waves Appl. **30**:473–491.

Choi, C. and Konrad, A. (1991). Finite element modeling of the RF heating process. IEEE Trans. Magn. **27**:4227–4230.

Datta, A. and Ni, H. (2002). Infrared and hot-air-assisted microwave heating of foods for control of surface moisture. J. Food Eng. **51**:355–364.

Datta, A. (2007). Porous media approaches to studying simultaneous heat and mass transfer in food processes. I: Problem formulations. J. Food Eng. **80**:80–95.

Dev, S. R., Kannan, S., Gariepy, Y. and Raghavan, V. G. (2012). Optimization of radiofrequency heating of in-shell eggs through finite element modeling and experimental trials. Prog. Electromagn. Res. **45**:203–222.

Dhall, A. and Datta, A. (2011). Transport in deformable food materials: a poromechanics approach. Chem. Eng. Sci. **66**:6482–6497.

Farag, K., Lyng, J., Morgan, D. and Cronin, D. (2008a). A comparison of conventional and radio frequency tempering of beef meats: effects on product temperature distribution. Meat Sci. **80**:488–495.

Farag, K., Lyng, J., Morgan, D. and Cronin, D. (2008b). Dielectric and thermophysical properties of different beef meat blends over a temperature range of −18 to +10°C. Meat Sci. **79**:740–747.

Farag, K., Duggan, E., Morgan, D., Cronin, D. and Lyng, J. (2009). A comparison of conventional and radio frequency defrosting of lean beef meats: effects on water binding characteristics. Meat Sci. **83**:278–284.

Farag, K., Lyng, J., Morgan, D. and Cronin, D. (2011). A comparison of conventional and radio frequency thawing of beef meats: effects on product temperature distribution. Food Bioprocess Technol. **4**:1128–1136.

Fu, Y. C. (2004). Fundamentals and industrial applications of microwave and radio frequency in food processing. **In**: *Food Processing: Principles and Applications*, pp.79–100. Smith, J. S. and Hui, Y. H., Eds., Blackwell, Iowa, USA.

Gao, M., Tang, J., Wang, Y., Powers, J. and Wang, S. (2010). Almond quality as influenced by radio frequency heat treatments for disinfestation. Postharvest Biol. Technol. **58**:225–231.

Gao, M., Tang, J., Villa-Rojas, R., Wang, Y. and Wang, S. (2011). Pasteurization process development for controlling *Salmonella* in in-shell almonds using radio frequency energy. J. Food Eng. **104**:299–306.

Geedipalli, S., Rakesh, V. and Datta, A. (2007). Modeling the heating uniformity contributed by a rotating turn3/17/2017 in microwave ovens. J. Food Eng. **82**:359–368.

Geveke, D. J., Kozempel, M., Scullen, O. J. and Brunkhorst, C. (2002). Radio frequency energy effects on microorganisms in foods. Innov Food Sci. Emerg Technol. **3**:133–138.

Guan, D., Cheng, M., Wang, Y. and Tang, J. (2004). Dielectric properties of mashed potatoes relevant to microwave and radio-frequency pasteurization and sterilization processes. J. Food Sci. **69**:30–37.

Ha, J. W., Kim, S. Y., Ryu, S. R. and Kang, D. H. (2013). Inactivation of *Salmonella enterica* serovar Typhimurium and Escherichia coli O157: H7 in peanut butter cracker sandwiches by radio-frequency heating. Food Microbiol. **34**:145–150.

Hartshorn, L. (1949). *Radio frequency heating*. George Allen & Unwin Ltd. London, UK.

Holland, J. M. (1974). Dielectric post baking in biscuit making. Bak Ind. J. **6**:169–176.

Hou, L., Ling, B. and Wang, S. (2014). Development of thermal treatment protocol for disinfesting chestnuts using radio frequency energy. Postharvest Biol. Tech. **98**:65–71.

Hou, L., Johnson, J. A. and Wang, S. (2016). Radio frequency heating for postharvest control of pests in agricultural products: A review. Postharvest Biol. Technol. **113**:106–118.

Huang, Z., Chen, L. and Wang, S. (2015a). Computer simulation of radio frequency selective heating of insects in soybeans. Int. J. Heat Mass Transfer. **90**:406–417.

Huang, Z., Zhu, H. and Wang, S. (2015b). Finite element modeling and analysis of radio frequency heating rate in mung beans. Trans. ASAE. **58**:149–160.

Huang, Z., Zhu, H., Yan, R. and Wang, S. (2015c). Simulation and prediction of radio frequency heating in dry soybeans. Biosyst. Eng. **129**:34–47.

Huang, Z., Marra, F. and Wang, S. (2016a). A novel strategy for improving radio frequency heating uniformity of dry food products using computational modeling. Innov Food Sci. Emerg Technol. **34**:100–111.

Huang, Z., Zhang, B., Marra, F. and Wang, S. (2016b). Computational modelling of the impact of polystyrene containers on radio frequency heating uniformity improvement for dried soybeans. Innov Food Sci. Emerg Technol. **33**:365–380.

Içier, F. and Baysal, T. (2004a). Dielectrical properties of food materials-1: factors affecting and industrial uses. Crit. Rev. Food Sci. Nutr. **44**:465–471.

Içier, F. and Baysal, T. (2004b). Dielectrical properties of food materials-2: Measurement techniques. Crit. Rev. Food Sci. Nutr. **44**:473–478.

Ikediala, J., Hansen, J., Tang, J., Drake, S. and Wang, S. (2002). Development of a saline water immersion technique with RF energy as a post-harvest treatment against codling moth in cherries. Postharvest Biol. Tech. **24**:209–221.

Jiao, S., Tang, J., Johnson, J., Tiwari, G. and Wang, S. (2011). Determining radio frequency heating uniformity of mixed beans for disinfestation treatments. Trans. ASAE. **54**:1847–1855.

Jiao, S., Johnson, J., Tang, J. and Wang, S. (2012). Industrial-scale radio frequency treatments for insect control in lentils. J. Stored Prod. Res. **48**:143–148.

Jiao, S., Deng, Y., Zhong, Y., Wang, D. and Zhao, Y. (2015a). Investigation of radio frequency heating uniformity of wheat kernels by using the developed computer simulation model. Food Res. Int. **71**:41–49.

Jiao, S., Zhu, D., Deng, Y. and Zhao, Y. (2016). Effects of hot air-assisted radio frequency heating on quality and shelf-life of roasted peanuts. Food Bioprocess Technol. **9**:308–319.

Jiao, Y., Tang, J. and Wang, S. (2014a). A new strategy to improve heating uniformity of low moisture foods in radio frequency treatment for pathogen control. J. Food Eng. **141**:128–138.

Jiao, Y., Tang, J., Wang, S. and Koral, T. (2014b). Influence of dielectric properties on the heating rate in free-running oscillator radio frequency systems. J. Food Eng. **120**:197–203.

Jiao, Y., Shi, H., Tang, J., Li, F. and Wang, S. (2015b). Improvement of radio frequency (RF) heating uniformity on low moisture foods with Polyetherimide (PEI) blocks. Food Res. Int. **74**:106–114.

Jojo, S. and Mahendran, R. (2013). Radio frequency heating and its application in food processing: A review. Int. J. Curr. Agric Res. **1**:42–46.

Jones, P. L. and Rowley, A. T. (1996). Dielectric drying. Drying Technol. **14**:1063–1098.

Jumah, R. (2005). Modelling and simulation of continuous and intermittent radio frequency-assisted fluidized bed drying of grains. Food Bioprod. Process. **83**:203–210.

Kim, S. Y., Sagong, H. G., Choi, S. H., Ryu, S. and Kang, D. H. (2012). Radio-frequency heating to inactivate *Salmonella* Typhimurium and *Escherichia coli* O157: H7 on black and red pepper spice. Int. J. Food Microbiol. **153**:171–175.

Kim, Y. R., Morgan, M., Okos, M. and Stroshine, R. (1998). Measurement and prediction of dielectric properties of biscuit dough at 27 MHz. J. Microw. Power EE. **33**:184–194.

Kirmaci, B. and Singh, R. K. (2012). Quality of chicken breast meat cooked in a pilot-scale radio frequency oven. Innov Food Sci. Emerg Technol. **14**:77–84.

Lau, S. K., Thippareddi, H., Jones, D., Negahban, M. and Subbiah, J. (2016). Challenges in radio frequency pasteurization of shell eggs: Coagulation rings. J. Food Sci. **81**:2492–2502.

Laycock, L., Piyasena, P. and Mittal, G. (2003). Radio frequency cooking of ground, comminuted and muscle meat products. Meat Sci. **65**:959–965.

Ling, B., Hou, L., Li, R. and Wang, S. (2016). Storage stability of pistachios as influenced by radio frequency treatments for postharvest disinfestations. Innov Food Sci. Emerg Technol. **33**:257–364.

Liu, C. M., Sakai, N. and Hanzawa, T. (1999). Three dimensional analysis of heat transfer during food thawing by far-infrared radiation. Food Sci. Technol. Res. **5**:294–299.

Liu, Q., Zhang, M., Xu, B., Fang, Z. and Zheng, D. (2015). Effect of radio frequency heating on the sterilization and product quality of vacuum packaged Caixin. Food Bioprod. Process. **95**:47–54.

Liu, Y., Tang, J. and Mao, Z. (2009). Analysis of bread dielectric properties using mixture equations. J. Food Eng. **93**:72–79.

Liu, Y., Tang, J., Mao, Z., Mah, J. H., Jiao, S. and Wang, S. (2011). Quality and mold control of enriched white bread by combined radio frequency and hot air treatment. J. Food Eng. **104**:492–498.

Liu, Y., Wang, S., Mao, Z., Tang, J. and Tiwari, G. (2013). Heating patterns of white bread loaf in combined radio frequency and hot air treatment. J. Food Eng. **116**:472–477.

Llave, Y., Terada, Y., Fukuoka, M. and Sakai, N. (2014). Dielectric properties of frozen tuna and analysis of defrosting using a radio-frequency system at low frequencies. J. Food Eng. **139**:1–9.

Llave, Y., Liu, S., Fukuoka, M. and Sakai, N. (2015). Computer simulation of radiofrequency defrosting of frozen foods. J. Food Eng. **152**:32–42.

Luechapattanaporn, K., Wang, Y., Wang, J., Al-Holy, M., Kang, D. H., Tang, J. and Hallberg, L. M. (2004). Microbial safety in radio frequency processing of packaged foods. J. Food Sci. **69**:201–206.

Luechapattanaporn, K., Wang, Y., Wang, J., Tang, J., Hallberg, L. M. and Dunne, C. P. (2005). Sterilization of scrambled eggs in military polymeric trays by radio frequency energy. J. Food Sci. **70**:288–294.

Marchand, C. and Meunier, T. (1990). Recent developments in industrial radio-frequency technology. J. Microwave Power EE. **25**:39–46.

Marra, F., Lyng, J., Romano, V. and McKenna, B. (2007). Radio-frequency heating of foodstuff: solution and validation of a mathematical model. J. Food Eng. **79**:998–1006.

Marra, F., Zhang, L. and Lyng, J. G. (2009). Radio frequency treatment of foods: review of recent advances. J. Food Eng. **91**:497–508.

Marra, F., De Bonis, M. V. and Ruocco, G. (2010). Combined microwaves and convection heating: A conjugate approach. J. Food Eng. **97**:31–39.

Marshall, M. and Metaxas, A. (1998). Modeling of the radio frequency electric field strength developed during the RF assisted heat pump drying of particulates. J. Microwave Power EE. **33**:167–177.

McCormick, R. (1988). Dielectric heat seeks low moisture applications. Prepared Foods. **162**:139–140.

Mermelstein, N. (1997). Interest in radio frequency heating heats up. Food Technol. **50**:94–95.

Metaxas, A. (1996). *Foundations of electroheat: a unified approach*. John Wiley & Sons, New York.

Moreira, R., Palau, J., Sweat, V. and Sun, X. (1995). Thermal and physical properties of tortilla chips as a function of frying time. J. Food Process Pres. **19**:175–189.

Moyer, J. and Stotz, E. (1947). The blanching of vegetables by electronics. Food Technol. **1**:252–257.

Nagaraj, G., Purohit, A., Harrison, M., Singh, R., Hung, Y. C. and Mohan, A. (2016). Radio frequency pasteurization of inoculated ground beef homogenate. Food Control. **59**:59–67.

Nelson, S. O. (2008). Dielectric properties of agricultural products and some applications. Res. Agric. Eng. **54**:104–112.

Nelson, S. O. and Trabelsi, S. (2012). Factors influencing the dielectric properties of agricultural and food products. J. Microw. Power EE. **46**:93–107.

Neophytou, R. and Metaxas, A. (1996). Computer simulation of a radio frequency industrial system. J. Microw. Power EE. **31**:251–259.

Neophytou, R. and Metaxas, A. (1997). Characterisation of radio frequency heating systems in industry using a network analyser. IEE P. Sci. Meas. Tech. **144**:215–222.

Neophytou, R. and Metaxas, A. (1998). Combined 3D FE and circuit modeling of radio frequency heating systems. J. Microw. Power EE. **33**:243–262.

Neophytou, R. and Metaxas, A. (1999). Combined tank and applicator design of radio frequency heating systems, IEEE P-Microw. Anten P. **146**:311–318.

Ni, H., Datta, A. K. and Torrance, K. E. (1999). Moisture transport in intensive microwave heating of biomaterials: a multiphase porous media model. Int. J. Heat Mass Transfer. **42**:1501–1512.

Orsat, V., Gariepy, Y., Raghavan, G. and Lyew, D. (2001). Radio-frequency treatment for ready-to-eat fresh carrots. Food Res. Int. **34**:527–536.

Pace, M., De Bonis, M. V., Marra, F. and Ruocco, G. (2011). Characterization of a combination oven prototype: Effects of microwave exposure and enhanced convection to local temperature rise in a moist substrate. Int. Commun. Heat Mass Transfer. **38**:557–564.

Pan, L., Jiao, S., Gautz, L., Tu, K. and Wang, S. (2012). Coffee bean heating uniformity and quality as influenced by radio frequency treatments for postharvest disinfestations. Trans. ASAE. **55**:2293–2300.

Pham, Q. T. (2006). Modelling heat and mass transfer in frozen foods: a review. Int. J. Refrig. **29**:876–888.

Piyasena, P., Dussault, C., Koutchma, T., Ramaswamy, H. and Awuah, G. (2003). Radio frequency heating of foods: principles, applications and related properties-a review. Crit. Rev. Food Sci. Nutr. **43**:587–606.

Rincon, A. M., Singh, R. K. and Stelzleni, A. M. (2015). Effects of endpoint temperature and thickness on quality of whole muscle non-intact

steaks cooked in a radio frequency oven. LWT — Food Sci. Technol. **64**:1323–1328.

Romano, V. and Marra, F. (2008). A numerical analysis of radio frequency heating of regular shaped foodstuff. J. Food Eng. **84**:449–457.

Ryynänen, S. (1995). The electromagnetic properties of food materials: a review of the basic principles. J. Food Eng. **26**:409–429.

Sahin, S., Sastry, S. and Bayindirli, L. (1999). Effective thermal conductivity of potato during frying: measurement and modeling. Int. J. Food Prop. **2**:151–161.

Shrestha, B. and Baik, O. D. (2013). Radio frequency selective heating of stored-grain insects at 27.12 MHz: a feasibility study. Biosyst. Eng. **114**:195–204.

Sisquella, M., Casals, C., Picouet, P., Viñas, I., Torres, R. and Usall, J. (2013). Immersion of fruit in water to improve radio frequency treatment to control brown rot in stone fruit. Postharvest Biol. Technol. **80**:31–36.

Sosa-Morales, M., Tiwari, G., Wang, S., Tang, J., Garcia, H. and Lopez-Malo, A. (2009). Dielectric heating as a potential post-harvest treatment of disinfesting mangoes, Part II: Development of RF-based protocols and quality evaluation of treated fruits. Biosyst. Eng. **103**:287–296.

Tang, J., Feng, H. and Lau, M. (2002). Microwave heating in food processing. **In**: *Advances in Bioprocessing Engineering*, pp. 1–43. New York: Scientific Press.

Tang, J., Wang, Y. and Chan, T. (2005). Radio frequency heating in food processing. **In**: *Novel Food Processing Technologies*, pp. 501–524. New York, NY: Marcel Dekker.

Tiwari, G., Wang, S., Birla, S. and Tang, J. (2008). Effect of water-assisted radio frequency heat treatment on the quality of 'Fuyu'persimmons. Biosyst. Eng. **100**:227–234.

Tiwari, G., Wang, S., Tang, J. and Birla, S. (2011a). Analysis of radio frequency (RF) power distribution in dry food materials. J. Food Eng. **104**:548–556.

Tiwari, G., Wang, S., Tang, J. and Birla, S. (2011b). Computer simulation model development and validation for radio frequency (RF) heating of dry food materials. J. Food Eng. **105**:48–55.

Uyar, R., Erdogdu, F. and Marra, F. (2014). Effect of load volume on power absorption and temperature evolution during radio-frequency heating of meat cubes: A computational study. Food Bioprod Process. **92**:243–251.

Uyar, R., Bedane, T. F., Erdogdu, F., Palazoglu, T. K., Farag, K. W. and Marra, F. (2015). Radio frequency thawing of food products-a computational study. J. Food Eng. **146**:163–171.

Uyar, R., Erdogdu, F., Sarghini, F. and Marra, F. (2016). Computer simulation of radio-frequency heating applied to block-shaped foods: Analysis on the role of geometrical parameters. Food Bioprod. Process. **98**:310–319.

Venkatesh, M. and Raghavan, G. (2005). An overview of dielectric properties measuring techniques. Can. Biosyst. Eng. **47**:15–30.

Wang, J., Olsen, R. G., Tang, J. and Tang, Z. (2008a). Influence of mashed potato dielectric properties and circulating water electric conductivity on radio frequency heating at 27 MHz. J. Microw. Power EE. **42**:31–46.

Wang, J., Luechapattanaporn, K., Wang, Y. and Tang, J. (2012). Radio frequency heating of heterogeneous food-meat lasagna. J. Food Eng. **108**:183–193.

Wang, S., Ikediala, J., Tang, J., Hansen, J., Mitcham, E., Mao, R. and Swanson, B. (2001). Radio frequency treatments to control codling moth in in-shell walnuts. Postharvest Biol. Technol. **22**:29–38.

Wang, S., Tang, J., Johnson, J., Mitcham, E., Hansen, J., Cavalieri, R., Bower, J. and Biasi, B. (2002). Process protocols based on radio frequency energy to control field and storage pests in in-shell walnuts. Postharvest Biol. Technol. **26**:265–273.

Wang, S., Tang, J., Cavalieri, R. and Davis, D. (2003a). Differential heating of insects in dried nuts and fruits associated with radio frequency and microwave treatments. Trans. ASAE. **46**:1175–1182.

Wang, S., Yue, J., Tang, J. and Chen, B. (2005). Mathematical modelling of heating uniformity for in-shell walnuts subjected to radio frequency treatments with intermittent stirrings. Postharvest Biol. Technol. **35**:97–107.

Wang, S., Birla, S., Tang, J. and Hansen, J. D. (2006a). Postharvest treatment to control codling moth in fresh apples using water assisted radio frequency heating. Postharvest Biol. Technol. **40**:89–96.

Wang, S., Tang, J., Sun, T., Mitcham, E., Koral, T. and Birla, S. (2006b). Considerations in design of commercial radio frequency treatments for postharvest pest control in in-shell walnuts. J. Food Eng. **77**:304–312.

Wang, S., Monzon, M., Johnson, J., Mitcham, E. and Tang, J. (2007a). Industrial-scale radio frequency treatments for insect control in walnuts: I: Heating uniformity and energy efficiency. Postharvest Biol. Technol. **45**:240–246.

Wang, S., Monzon, M., Johnson, J., Mitcham, E. and Tang, J. (2007b). Industrial-scale radio frequency treatments for insect control in walnuts: II: Insect mortality and product quality. Postharvest Biol. Technol. **45**:247–253.

Wang, S., Luechapattanaporn, K. and Tang, J. (2008b). Experimental methods for evaluating heating uniformity in radio frequency systems. Biosyst. Eng. **100**:58–65.

Wang, S., Yue, J., Chen, B. and Tang, J. (2008c). Treatment design of radio frequency heating based on insect control and product quality. Postharvest Biol. Technol. **49**:417–423.

Wang, S., Tiwari, G., Jiao, S., Johnson, J. and Tang, J. (2010). Developing postharvest disinfestation treatments for legumes using radio frequency energy. Biosyst. Eng. **105**:341–349.

Wang, S., Tang, J., Johnson, J. and Cavalieri, R. (2013). Heating uniformity and differential heating of insects in almonds associated with radio frequency energy. J. Stored Prod. Res. **55**:15–20.

Wang, Y., Wig, T., Tang, J. and Hallberg, L. (2003b). Sterilization of foodstuffs using radio frequency heating. J. Food Sci. **68**:539–544.

Wang, Y., Li, Y., Wang, S., Zhang, L., Gao, M. and Tang, J. (2011). Review of dielectric drying of foods and agricultural products. Int. J. Agric. & Biol. Eng. **4**:1–19.

Wang, Y., Zhang, L., Gao, M., Tang, J. and Wang, S. (2014). Pilot-scale radio frequency drying of macadamia nuts: Heating and drying uniformity. Drying Technol. **32**:1052–1059.

Yang, J., Zhao, Y. and Wells, J. H. (2003). Computer simulation of capacitive radio frequency (RF) dielectric heating on vegetable sprout seeds. J. Food Proc. Eng. **26**:239–263.

Zhang, H. and Datta, A. K. (2001). Electromagnetics of microwave heating: magnitude and uniformity of energy absorption in an oven. In: *Handbook of Microwave Technology for Food Applications*, pp. 1–28. Datta, A. K. and Anantheswaran, R. C., Eds., Marcel Dekker, New York.

Zhang, L., Lyng, J. G. and Brunton, N. P. (2004). Effect of radio frequency cooking on the texture, colour and sensory properties of a large diameter comminuted meat product. Meat Sci. **68**:257–268.

Zhao, Y., Flugstad, B., Kolbe, E., Park, J. W. and Wells, J. H. (2000). Using capacitive (radio frequency) dielectric heating in food processing and preservation-a review. J. Food Proc. Eng. **23**:25–55.

Zheng, A., Zhang, B., Zhou, L. and Wang, S. (2016). Application of radio frequency pasteurization to corn (*Zea mays L.*): Heating uniformity improvement and quality stability evaluation. J. Stored Prod. Res. **68**:63–72.

Zhou, L., Ling, B., Zheng, A., Zhang, B. and Wang, S. (2015). Developing radio frequency technology for postharvest insect control in milled rice. J. Stored Prod. Res. **62**:22–31.

Zhou, L. and Wang, S. (2016). Verification of radio frequency heating uniformity and Sitophilus oryzae control in rough, brown and milled rice. J. Stored Prod. Res. **65**:40–47.

Zhu, H., Huang, Z. and Wang, S. (2014). Experimental and simulated top electrode voltage in free-running oscillator radio frequency systems. J. Electromag. Waves Appl. **28**:606–617.

Zhu, J. F., Liu, J. Z., Wu, J. H., Cheng, J., Zhou, J. H. and Cen, K. F. (2015). Thin-layer drying characteristics and modeling of Ximeng lignite under microwave irradiation. Fuel Process. Technol. **130**:62–70.